Confocal optical microscopy

1996 Rep. Prog. Phys. 59 427

(http://iopscience.iop.org/0034-4885/59/3/003)

Rep. Prog. Phys. **59** (1996) 427–471. Printed in the UK

Confocal optical microscopy

Robert H Webb

Schepens Eye Research Institute and Wellman Laboratories of Photomedicine, Massachusetts General Hospital, Boston, MA 02114, USA

Abstract

Confocal optical microscopy is a technique for increasing the contrast of microscope images, particularly in thick specimens. By restricting the observed volume, the technique keeps overlying or nearby scatterers from contributing to the detected signal. The price for this is that the instrument must observe only one point at a time (in the scanning laser version) or a group of separated points with very little light (in the disc version). This paper describes how the confocal advantage comes about and how it is implemented in actual instruments.

This review was received in October 1995

0034-4885/96/030427+45$59.50

Contents

1. Theory

1.1. A simple view

Before getting into real detail I want to show a simple picture of the confocal process that all of us fall back on from time to time. Figure 1, in the first panel, shows how a lens forms an image of two points in a thick sample, one at the focal point and one away from that point. In the second panel a pinhole conjugate to the focal point passes all the light from the focal point, and very little of the light from the out-of-focus point. Panel 3 uses a light source confocal to the existing focus to shine intense light on the 'good' point and very little on the 'bad' one.

In many ways that is all there is to confocal microscopy. However, I want to show how all this comes about: the selection of light from one point and the rejection of light from all other points leads to the very high contrast images of confocal microscopy. That increase in contrast happens even when the imaged point is buried deep in a thick sample and is surrounded by other bright points. In the second part of the paper, on implementations, I will show how a single image of a confocal point can be used to look at a whole plane within the sample.

1.2. Microscopy

This paper is about optical confocal microscopy, a subset of the extensive and well developed field of microscopy. I will speak briefly of microscopes, to fix the terminology and to illustrate the differences in the later sections, but I urge the reader not to treat this as a complete description of a microscope. The paper by Inoué and Oldenbourg [1] and Inoué's book on video microscopy [2] are good general references for microscopy. Modern microscope development has included electron and acoustic microscopes, tunnelling and near-field imagers and even the machines of high-energy physics and radio astronomy. Contributions from these fields are well worth the attention of the student.

1.2.1. Components. Figure 3 shows the basic components of a microscope. This thin lens schematic shows the two optical systems that reside in any instrument. One system is the set of planes conjugate to the object, and therefore to the image. The other system is the set of planes conjugate to the pupil or lens aperture. The cross-hatched beam shows light from a single point on the object, reimaged in front of the ocular and then again on the detector—here the retina of an eye. The shoulder of the objective lens is a good estimated position for the (exit) pupil. It has been typical to make microscope tube lengths 160 mm from the shoulder. Then the first real image of the object lies 10 mm inside the tube, at 150 mm from the shoulder. Newer objective lenses may be 'infinity corrected', which means that they work with collimated light at the (exit) pupil, and need an extra lens (the tube lens) to meet the 150 mm requirement. Here the objective lens has an infinite conjugate, so it is followed by a tube lens to form an intermediate image at 150 mm. The ocular acts as a relay to yet another image plane—where there may be film, video camera or retina.

The second set of conjugate planes is that of the pupil. In the sketch the thick lines represent the extreme rays from the centre of the pupil—they cross at the image of the pupil. Analysis of a microscope by these two sets of conjugates is particularly felicitous

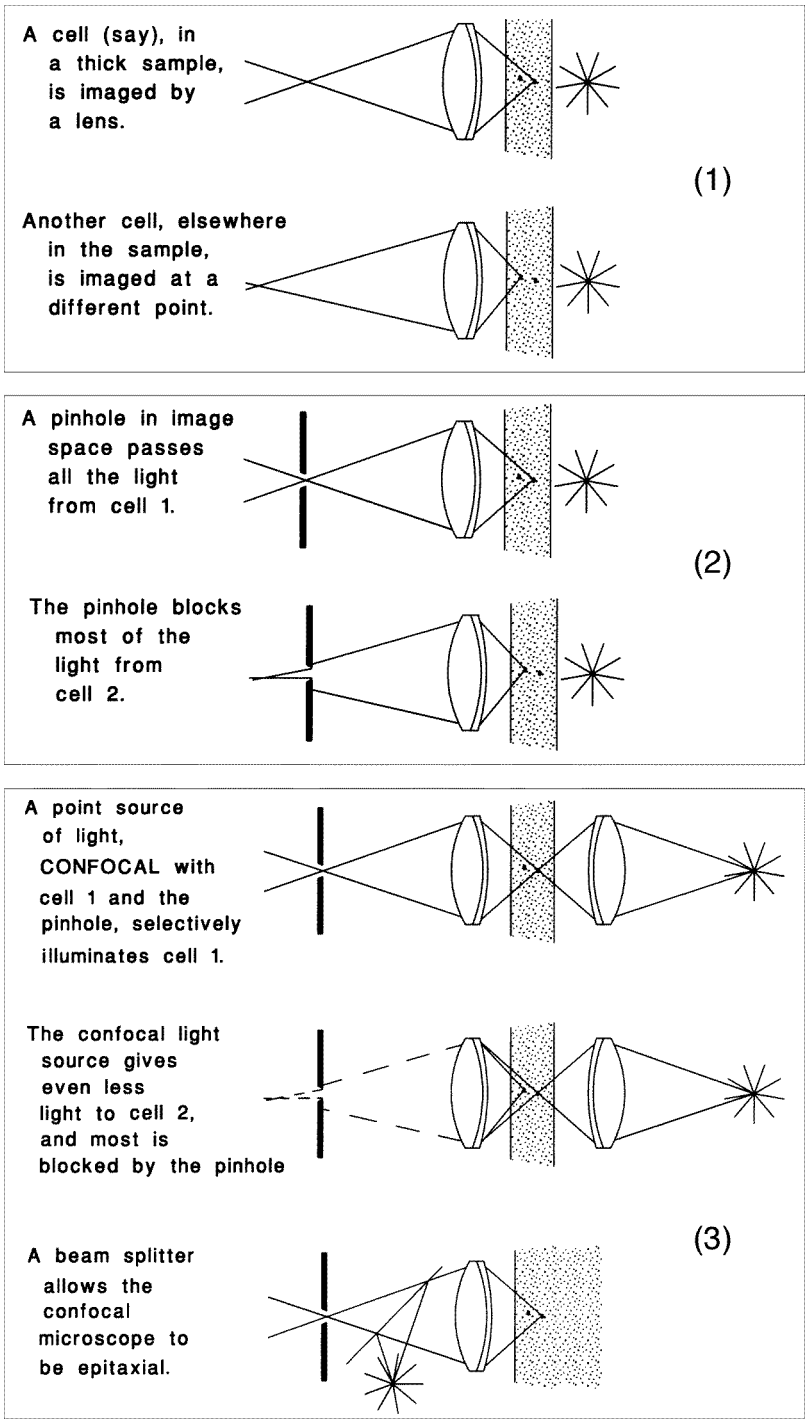

Figure 1. A simple view of the progression from wide field imager to confocal microscope.

for confocal microscopy: the cross-hatched pattern can represent the instantaneous position of the scanning beam. The thick lines show the extreme positions of that beam, pivoting at the pupils.

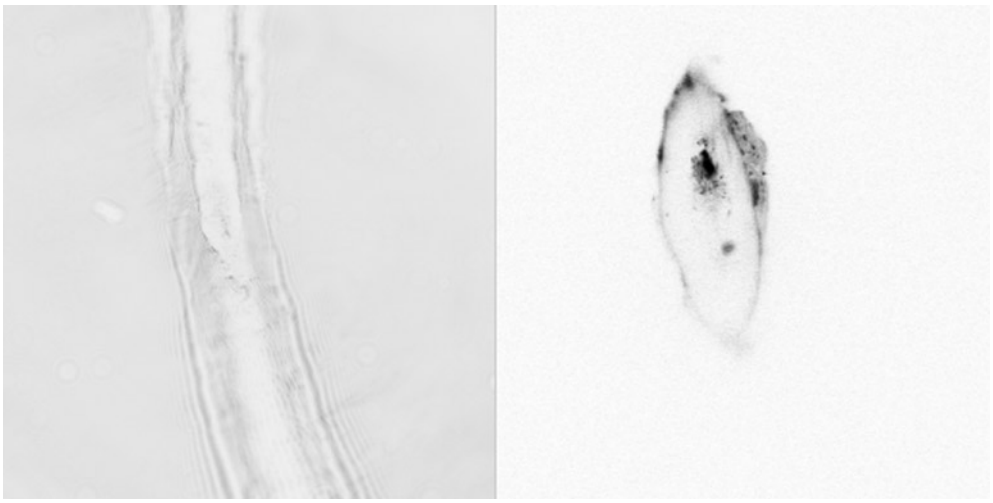

Figure 2. A single hair in wide field and confocal images. In the wide field image, on the left, the hair emerges from the paper from top to bottom. The confocal image, on the right, demonstrates optical sectioning: only the intersection of the focal plane with the hair is visible.

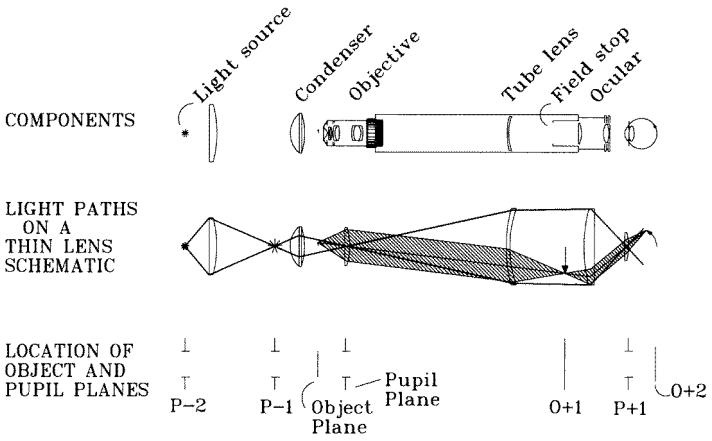

Figure 3. Schematic of a generalized microscope. The optical paths are shown on a thin lens plot to emphasize that the limits of the illuminated field are minima at the conjugates of the pupil. The cross-hatched beam shows light from one object point going to an intermediate image and then to the real image on a detector (the viewer's retina). Pupil conjugates are shown on the third line as stylized apertures. Planes conjugate to the image are indicated there by straight lines.

In Köhler illumination the lamp filament is conjugate to (imaged on) the pupillary planes, so that the conjugates to the object plane will be uniformly lit.

The objective lens is the critical element in every microscope. The objective lens determines magnification, field of view and resolution, and its quality determines light transmission and the contrast and aberrations of the image. These parameters and qualities are also critical in confocal microscopy, so a good objective lens is always necessary.

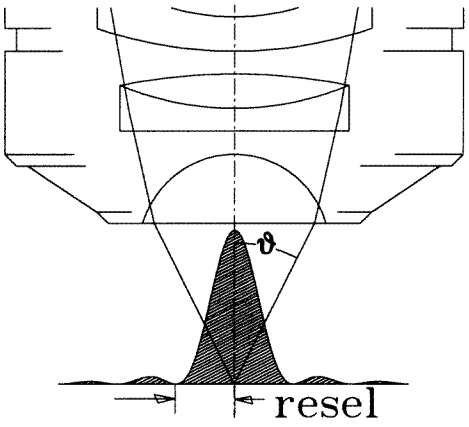

Figure 4. The resolution element due to a lens of $\mathrm{NA} = n \sin \vartheta$ is called a resel: the radius of the first dark fringe in the diffraction pattern, or half the diameter of the Airy disc.

Figure 4 illustrates the field of view and the diffraction-limited resolution due to the finite aperture of the objective lens. If some other aperture in a plane conjugate to the pupil is smaller than the pupil of the objective lens, then that smaller aperture will control the resolution. For most microscopes (and indeed for most optical devices) the field of view is less than 1000 resolution elements [3].

1.2.2. Illumination. Illumination in an optical microscope includes anything that can shine photons on the object. This includes sources with wavelengths from the ultraviolet (say 250 nm) to the far infrared (~ 3 μm), with incoherent white light from incandescent filaments being the most common. Lasers have high radiance and are monochromatic. Their coherence leads to differences in imaging that are the subject of extensive exploration. Conventional microscopes generally use incoherent illumination, and are analysed accordingly. Coherent illumination generally causes trouble in microscopy because unwanted interference effects degrade the images. I will be discussing illumination with laser light, which is highly coherent, but I will treat it as incoherent. This is appropriate because the illumination will be a focused beam that moves. Therefore when one spot is illuminated no other nearby spots are illuminated, and interference cannot occur. A consequence of this is that there can be no *speckle* effects with a scanning laser imager, and speckle is not a problem in confocal microscopy.

Light may fall on the object from the side opposite the observer, as shown in figure 3, or it may be *epitaxial*, which means that it comes from the observation side. Epitaxial illumination is used for viewing opaque and fluorescent objects. An opaque material such as a semiconductor chip has to be seen by light scattered and reflected from its surface. I will use the general term *remitted* to mean both scattered and reflected. Fluorescent objects appear with high contrast because they are seen in light of a wavelength longer than that of the illumination, and any illumination light can be rejected. Most confocal microscopes are epitaxial—for these reasons and for the parsimony of using one objective lens twice.

1.2.3. Mode. There are many arrangements of the illumination and observation geometries that are variants of the simple arrangement of figure 3. Each of these is useful for specific situations, and many are used regularly by microscopists. *Dark field* refers to illumination from one angle and observation from another, emphasizing deflected or scattered light over reflected or absorbed light. *Phase contrast* is a technique for displaying differences in optical

path length that may not result in absorption or deflection, but rather cause a difference in the phase of the wavefront. This is essentially an interference technique, primarily to see spatial variations in transparent objects. DIC (differential interference contrast) is a mode in which a shearing interferometer subtracts the amplitude (not intensity) of an image from a slightly displaced copy to emphasize the areas of changing index or optical path. *Nomarski* mode uses polarization to accomplish the same task. Most microscopists know and use some of these and various other interference techniques on a regular basis.

1.2.4. Recording. Microscope images are recorded on a variety of media, with the retina of the eye and photographic film being the most common until recently. Now the list includes video cameras—often used in still mode for long integrations—and electronic detectors recording one point of the object at a time. For confocal microscopy all recording media are relevant, though the electronic ones will take up most of my attention.

1.2.5. Descriptors. Microscopists generally describe their instruments in specialized terms—most of which refer to the objective lens. Such distinctions as apochromats and aplanatic surfaces determine the control of aberrations and are important in the choice of objective lenses for a given task, but do not change for confocal microscopy. I will use the mathematical descriptors that are common in describing resolution and contrast, and leave the special descriptors of objective lenses to the references. Figures 4 and 5 demonstrate the *numerical aperture* (NA) of a lens.

$$\mathrm{NA} = n \sin \vartheta \tag{1}$$

where n is the index of refraction of the medium and (ϑ is the half angle of the cone of light converging to an illuminated spot or diverging from one. NA describes the angular behaviour of the light cone, and it is that which governs the imaging. Physicists tend to use the f-number ($f/\#$) to describe that convergence or divergence cone:

$$f/\# = n/2\mathrm{NA}\,. \tag{2}$$

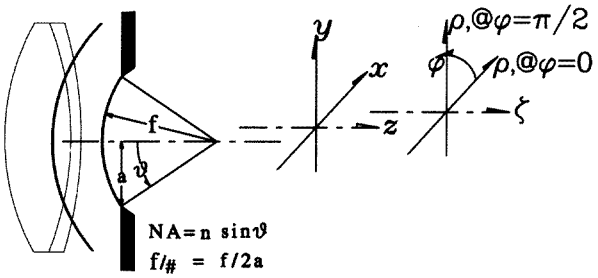

Figure 5. Numerical aperture (NA) and f-number ($f/\#$) are illustrated here for a converging spherical wavefront. The optic axis is taken along z, which is scaled to ζ and the planes of constant ζ contain the scaled radius ρ and the azimuth φ.

A proper metric in object space is the wavelength of the measuring light, λ in vacuum or λ/n in a medium of index n. For convenience of scaling I will use a reduced variable along z, the optic axis, that I will call ζ (zeta), and a radial variable perpendicular to the axis, called ρ (rho).

Scaling of the z dimension, along the optic axis, is

$$\zeta(r) = \frac{2\pi}{n\lambda}\mathrm{NA}^2 z = 2\pi\frac{n}{\lambda}z\sin^2\vartheta = z\boldsymbol{k}'\sin^2\vartheta\ . \tag{3}$$

For some readers it will be more familiar to use $\boldsymbol{k}' = 2\pi n/\lambda$.

In the plane transverse to the optic axis the scaled dimension is

$$\rho(r) = \frac{2\pi}{\lambda}r\mathrm{NA} = 2\pi\frac{n}{\lambda}r\sin\vartheta = r\boldsymbol{k}'\sin\vartheta\ . \tag{4}$$

The quantities ρ and ζ are often called *optical units*, or *o.u.* Many authors follow Born and Wolf [4], chapter 8.8, who use

$$v \equiv \rho \qquad \text{and} \qquad u \equiv \zeta\ . \tag{5}$$

For a microscope of NA = 1, at 633 nm in water, $\rho = 10r$, and $\zeta = 7.5z$.

1.3. Contrast and resolution

The two components of image quality are contrast and resolution. Resolution is one of those clean concepts in physics that can be described, measured and manipulated according to rules derived from the geometry of the system. Contrast, on the other hand, is the noisy reality of real measurements that limits our ability to use the available resolution. I will start here with the definitions and groundwork for resolution, then describe how contrast modifies the actual image. My point of view throughout this review will be that confocal microscopy is one of the means by which we increase contrast so that the image more faithfully exhibits the available resolution. A confocal microscope does have slightly higher resolution than a wide field microscope, but this is not the source of most of its success.

1.3.1. Resolution. Point-spread function—usually. Figure 4 shows the intensity pattern illuminated or observed by a lens at its focal plane. That pattern is called the *point-spread function* (psf), and defines the *resel*, the resolution element transverse to the optic axis. For the most common approximations the psf at $\zeta = 0$ has the mathematical form $2J_1^2(\rho)/\rho^2$ for a circular aperture: this is the familiar Airy disc [5]. The common approximation is for paraxial optics, that is, the NA must be small! That is not a happy approximation for microscopy, but it is the one usually used. I show the function without approximation in appendix A, and details of the derivation are found in the paper by Richards and Wolf [6]. Hell and Stelzer [7] use this correct description†. The differences as NA becomes large should not be emphasized too much, since the general form of the function is unchanged. The main difference is that dark fringes never quite go to zero and that the width of the point-spread function is a bit more than the approximation predicts.

The psf is a function in three dimensions, but usually lenses and apertures are rotationally symmetric about the ζ axis and I will assume all directions perpendicular to ζ are the same and represented by ρ. (There is already an extensive literature on the effect of aberrations in confocal microscopy [8], but even that does not generally address the lack of rotational symmetry.) Along the optic axis the psf has the form $\left(\sin\frac{\zeta}{4}/\frac{\zeta}{4}\right)^2$ for the paraxial approximation. The point-spread function in the ζ, ρ plane is shown in figure 6—for small NA this is the much copied Linfootprint of Born and Wolf in the section cited. We will see later how the psf changes for confocal optics.

† Equation (2) has a misprint—see appendix A here.

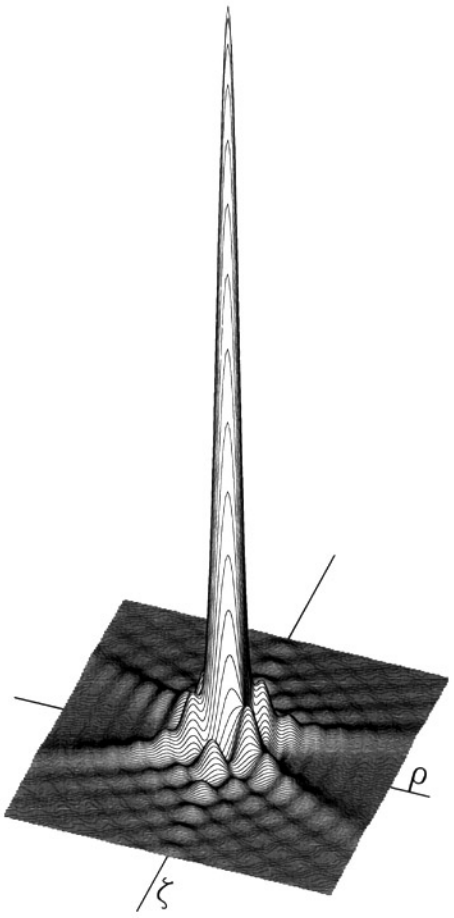

Figure 6. The function $p(\zeta, \rho)$ between zeta $= \pm 24\pi$ and $\rho = \pm 7\pi$ (6 resels).

In the focal plane ($\zeta = 0$) the point-spread function is $p(0, \rho) = 2J_1^2(\rho)/\rho^2$. Figure 8($a$) shows the pattern in the focal plane and other planes transverse to the optic axis. Along the optic axis, $p(\zeta, 0) = \left(\sin \frac{\zeta}{4} / \frac{\zeta}{4}\right)^2$, the diffraction pattern of a slit.

The integrated intensity in every transverse plane is the same. This means

$$\int_0^\infty p\,(\zeta, \rho)\rho\,\mathrm{d}\rho = \text{constant for any } \zeta, \tag{6}$$

every plane parallel to the focal plane makes an equal contribution to this integral, not surprising since the same energy flux passes each plane.

The term *point-spread function* (psf) usually refers to the pattern $p(0, \rho)$, but I am going to use it more generally to refer to the three-dimensional pattern $p(\zeta, \rho)$, as depicted in figures 6 and 8. The psf is the diffraction pattern due to a (circular) aperture, as brought to a focus by a lens. The amplitude diffraction pattern, $a(\zeta, \rho)$, carries phase information, and $p(\zeta, \rho) = a(\zeta, \rho) \times a^*(\zeta, \rho) = |a(\zeta, \rho)|^2$. The function $a(\zeta, \rho)$ is the Fourier transform of the aperture.

I use the term resel for the size of the transverse pattern in the focal plane, and define the resel as half the separation of the first dark fringes. The central portion, one resel in

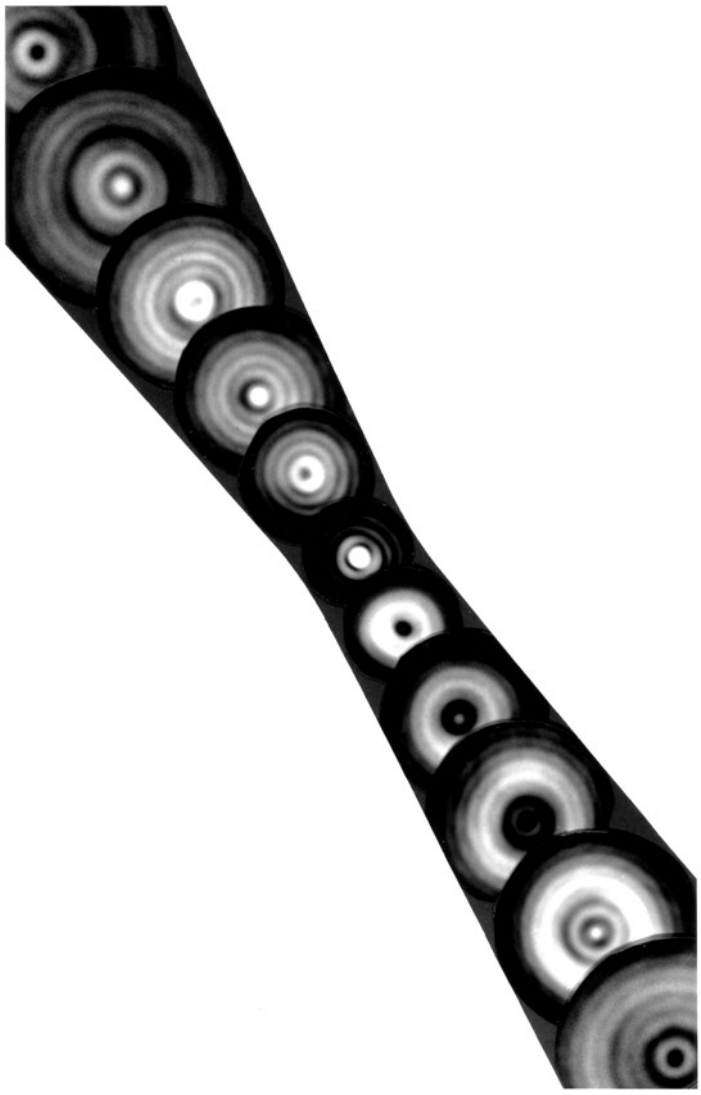

Figure 7. The point-spread function in through-focus series. Each sub-picture is from a plane parallel to the focal plane. These are actual photographs as a microscope is stepped through focus. Intensity has been manipulated, since the centre of the in-focus panel is really 100 times brighter than any of the others.

radius, is the Airy disc. The radius of the first dark fringe is

$$\rho_{\text{resel}} = 1.22\pi, \tag{7}$$

or

$$r_{\text{resel}} = 0.61\lambda/n \sin\vartheta\,. \tag{8}$$

I prefer to use the form

$$\boxed{r_{\text{resel}} = 1.22\lambda' f/\#,} \tag{9}$$

where $\lambda' = \lambda/n$.

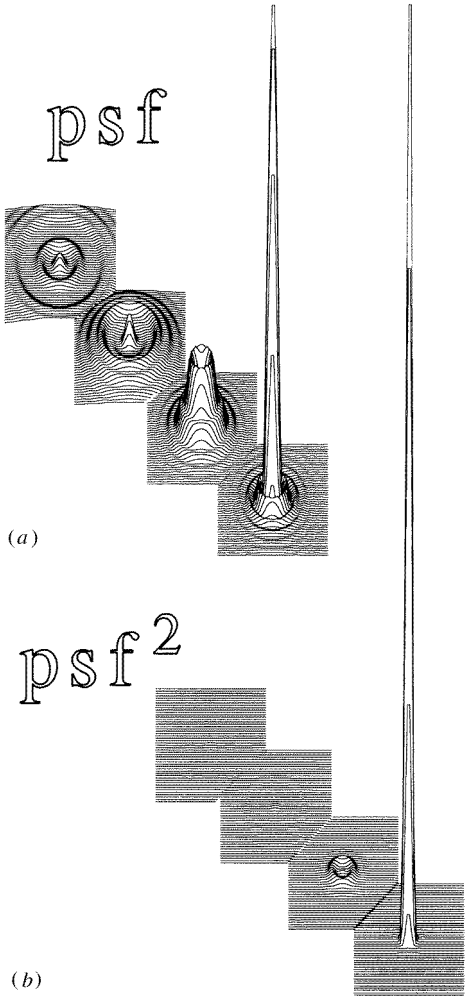

Figure 8. $p(\zeta, \rho)$ for the focal plane and planes parallel to it: in (*a*) this is for the conventional diffraction pattern, and in (*b*) it is for the confocal case.

Point-spread function—Gaussian beam. The concept of numerical aperture and the psf shown above assumes that the pupil of the objective lens limits the light. That means that the illumination overfills the pupil with a uniform irradiance. Laser illumination does not meet these criteria. A laser beam has a Gaussian cross section in intensity, and is specified by its half or $1/e^2$ power points.

$$I(\rho) = I_0 \, e^{-2\rho^2/w^2}, \tag{10}$$

where w is the parameter describing the beam width, usually called the 'beam waist' but referring to the beam *radius* at $1/e^2$.

If such a beam underfills the lens pupil it will be focused to a beam waist that is Gaussian in cross section. A partially filled pupil will produce a mixture of the Gaussian and diffraction patterns. Then by underfilling the pupil we can avoid all the complexity of the diffraction pattern and get much more light through, at the cost of a slight decrease in resolution. Figure 9 demonstrates this for pupils uniformly filled (flat) or cutting the Gaussian profile at $\frac{1}{2}$, 1 or $2.5w$. A match at the $1/e^2$ points—pupil edge at w—loses only 14% of the light and spoils the resolution very little. We generally want to use all the laser light we paid for.

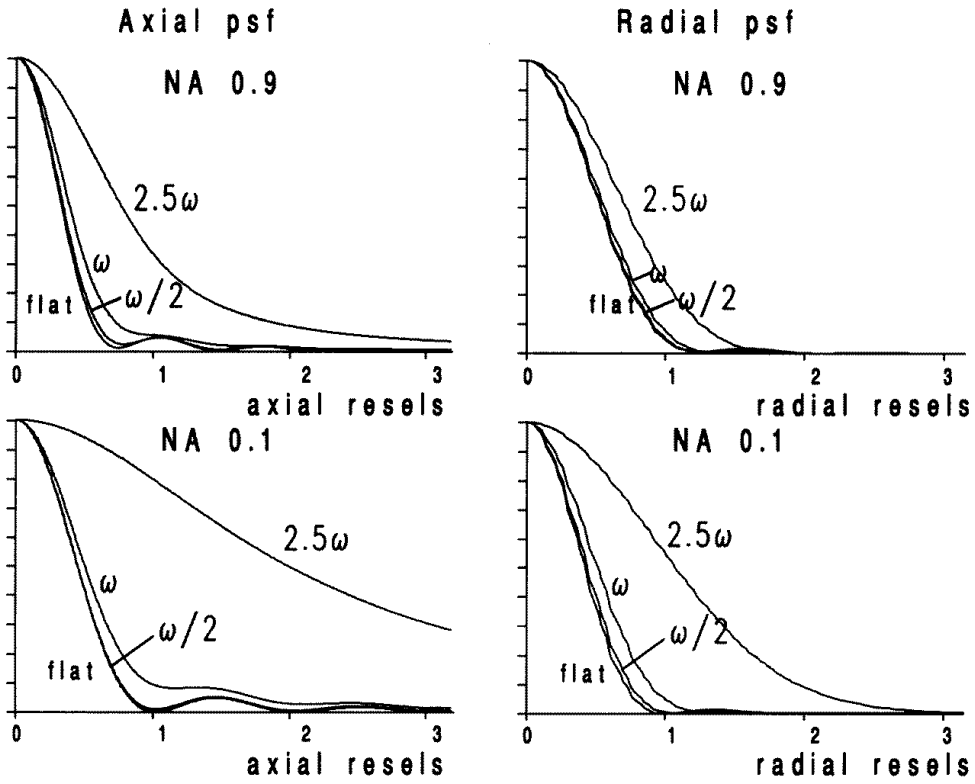

Figure 9. $p(\zeta,0)$ and $p(0,\rho)$ for two objective lenses: NA = 0.1 and NA = 0.9, and for four ratios of the Gaussian beam diameter to the pupil size. At w the pupil radius equals the $1/e^2$ point on the beam profile, so 86% of the energy gets through the pupil. One radial resel is $\Delta r = 1.22\lambda' f\#$, and one axial resel is $\Delta z = 6\lambda' f\#^2$, as we will see later.

Resolution. The psf is a measure of resolution because two self-luminous points viewed by a microscope appear separate only if they are far enough apart for their psf's to be distinct. Both self-luminous points display the diffraction patterns of equation (A9) in appendix A and so will be distinct only if they are far enough apart to display a reasonable dip between the two peaks. In figure 10 such a pair is shown, separated by one resel. That separation is the one suggested by Rayleigh [9] as 'resolved': the dip is about 26%. Figures 10 and 11 show the two points in three different presentations.

There is nothing about resolution that is limited to microscopy—equation (A9) applies to two stars in a telescope, for instance. Only the wavelength and the geometry of the defining aperture are involved, without any other parameters. We might, however, ask if Rayleigh chose the 'right' resolution criterion. Surely we can see a 1% dip, so that ought to be allowable. But, in fact, real images have noise, so a 1% dip will not be discernible in most real situations. We should be able to define how the resolution depends on noise—something like 'a d% dip is needed for an image with n% noise, so the separation would have to be $1/r$ resels'. This is where contrast enters the resolution picture.

1.3.2. Contrast. The 'dip' we need to resolve two points can be characterized by its intensity relative to the bright peaks. I will call that relative intensity *contrast*:

$$C = (n_b - n_d)/2n_{avg}, \tag{11}$$

where n_b is the intensity of the bright portions and n_d the intensity of the dim one. I have used $2n_{avg}$ as the denominator to agree with Michelson's [10] 'visibility' of fringes ($2n_{avg} = n_b + n_d$ in his terms). Noise decreases with averaging, so I must also define the size of the 'portion' that the n's come from. The image is divided into *pixels* for purposes of measurement. These are not the same as resels, which come from the optics, but rather they are the divisions of the measuring device. A CCD TV camera divides (pixellates) its image because it is an array of photosensitive areas of the silicon chip. Eyes and photographic film introduce pixellations too—in fact, there are no detectors which are infinitely small, so images are never free of pixellation effects [11]. For our purposes here we need only state the result from sampling theory: in order for the image to reproduce the object faithfully there must be at least two pixels per resel in every dimension. That requirement is known as the Nyquist criterion, and applies generally to any sampling process. The sampling requirement is slightly circular as I have stated it: the definition of resel might depend on contrast and the contrast might affect the definition of pixel. However, the circularity is second order, so we will proceed.

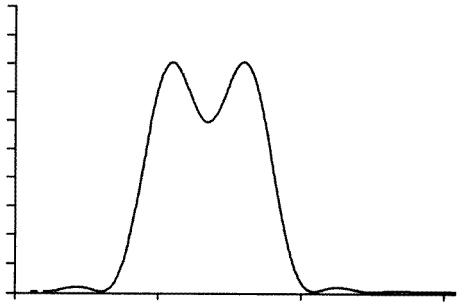

Figure 10. Two equal points separated by one resel illustrate the Rayleigh criterion for resolution.

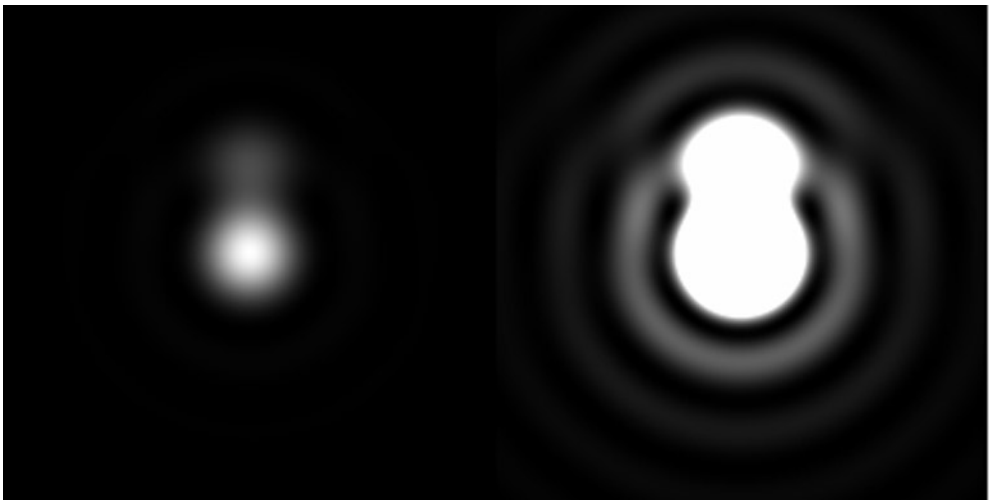

Figure 11. The display of figure 10 as intensity. The two points have unequal intensity, and the secondary diffraction maxima are visible only in the very overexposed frame, on the right.

Figure 12 shows the points of figure 10, but now with noise added. The pixel needs to be large enough to smooth the noise, but small enough not to degrade the resolution. Worse, in figure 13 the two points are shown having different intrinsic brightnesses, so that even without noise they may not appear distinct.

And now the truth comes out: it is not really contrast, but *noise* that determines visibility. Contrast is the term generally used, but in the backs of our minds we recognize that the problem is really noise. A page may be readable by daylight, but not by starlight. Truly black print reflects about 5% of the light falling on it ($n_d = 0.05n_b$) so the contrast in each case is $C = 0.9$, but there are too few photons by starlight. The irreducible limit on noise is that due to the random arrival times of the photons—the so-called *photon noise* or *quantum noise*. If my detector gives such a quantum-limited signal, the noise is proportional to the square root of the number of photons. That is, the number of photons falling on each detector pixel in each detector integration (sampling) time. So

$$\text{noise} = \sqrt{\text{number of photons}}\,. \tag{12}$$

Now contrast can be included. The actual number of photons n_b and n_d are what matter (as opposed to voltages, $v \propto n_b$, say. The *signal* for any pixel is

$$S \propto n_b - n_d, \tag{13}$$

where the n's are the numbers of photons. Then the noise for that pixel is

$$N \propto \sqrt{n_{avg}}, \tag{14}$$

so the pixel signal-to-noise ratio is

$$\text{SNR} = (n_b - n_d)/\sqrt{n_{avg}} = C\sqrt{n_{avg}}\,. \tag{15}$$

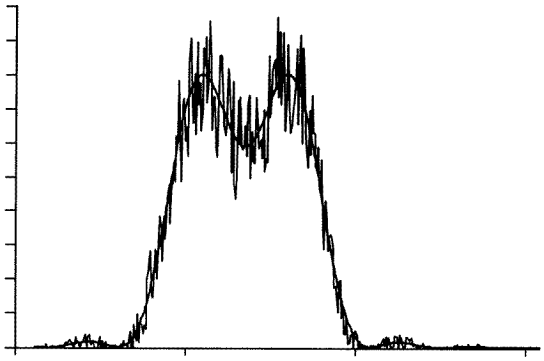

Figure 12. Two noisy equal points are still resolved according to the Rayleigh criterion, but we may not be able to see the dip.

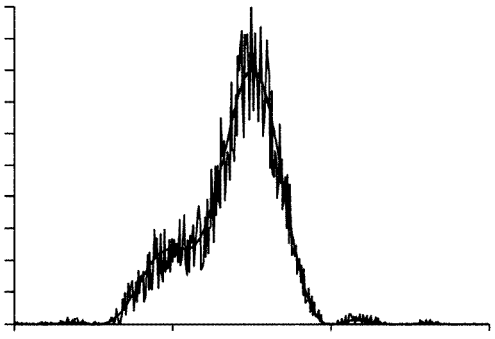

Figure 13. Two points separated by one resel, but of different brightness and obscured by noise. These may not be resolvable at this one resel separation.

The point of all this is that the visibility of the signal depends both on the contrast and on the general illumination level. In starlight the page with $C = 0.9$ has SNR $\cong \sqrt{n_{\text{avg}}}$, which is pretty small. Equation (15) shows that we want both high contrast and many photons, parameters that may be independent under ideal conditions. The number of photons depends on the illuminating power and the efficiency of the collection optics, while contrast is a feature of the object and of the way the microscope geometry excludes stray light. By *stray light* I mean light that is additive without being part of the signal: light that is the same for all nearby pixels. If we made some distinction between stray and relevant light, we might divide n_{b} and n_{d} into parts: $n_{\text{b}} = b + B$ where B is the general background light (the stray light) and $n_{\text{d}} = d + B$. Then contrast would be

$$C = \frac{b - d}{\sqrt{b^2 + d^2 + 2B^2}}, \tag{16}$$

and the $\sqrt{n_{\text{avg}}}$ in equation (15) includes all that unwanted light: $n_{\text{avg}} = \frac{1}{2}\sqrt{b^2 + d^2 + 2B^2}$. Microscopists have made every effort to reduce the unwanted contribution to the detected light. That reduction is generally included in the term 'contrast enhancement', but I will try to preserve the distinction of stray light reduction as a means of reducing noise. Because of the importance of this stray light term, I will rewrite the signal and noise equations explicitly,

$$S = n_{\text{b}} - n_{\text{d}}, \tag{17}$$

and

$$N = \sqrt[4]{n_{\text{b}}^2 + n_{\text{d}}^2 + 2n_{\text{stray}}^2}\,. \tag{18}$$

In the all-too-frequent case in which it is the background light that dominates, equation (15) becomes

$$\text{SNR} = 0.84(n_{\text{b}} - n_{\text{d}})/\sqrt{n_{\text{stray}}}\,. \tag{19}$$

The point of this complexity is that an effort to reduce stray background light can pay off. Most of the microscope modes described in section 1 reduce stray background light. For instance, phase contrast uses only light that has been retarded in phase by passage through the object, and fluorescence imaging uses only light that has been shifted in frequency. Confocal microscopes use only light that comes from the volume of the object conjugate to the detector and the source. Once the background light has been reduced, the full resolution available from the optics may be realized. A complete treatment appears in the paper by Sandison [12].

1.3.3. Scanning to improve contrast. 'Scanning' is the term used to describe sequential illumination or sequential observation of small areas of something. Thus a television monitor 'scans' its beam of electrons over the surface of the cathode ray tube. And a radar scans its microwave beam and reception pattern over nearby airspace or distant planets. The advantage of scanning is that, to first order, no energy reaches the detector from areas not in the beam, and so the contrast is not spoiled by unwanted background photons. A stationary beam and moving object is a form of scanning. This kind of contrast enhancement is at the heart of confocal microscopy, with the optics specialized to maximize the effect and to allow observation along the beam. The following sections will discuss such special optics, the increased resolution that is a (perhaps incidental) consequence of the optics, and various ways that the essential scanning is accomplished.

1.4. Confocal

Observation from the side, as in the Tyndall effect, is awkward in microscopy. Rather, we want to look along the direction of the beam and see only the volume around the focal area. Figure 14 shows how it is possible to view only the focal volume. In this schematic the scanning is halted to look at one beam position (or one instant). A point light source is imaged at the object plane, so that the illuminated point and the source are confocal. Then the observation optics form an image of the illuminated point on a pinhole. Now there are three points all mutually confocal—hence the name.

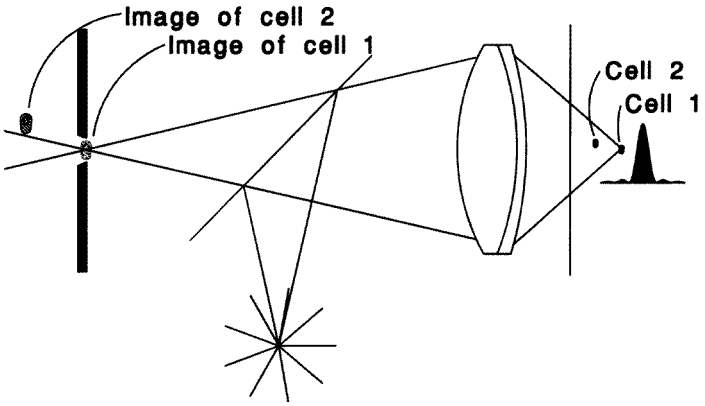

Figure 14. Light from a point source is imaged at a single point of the object and that, in turn, is imaged on a small pinhole, making all these points 'confocal'. Only entities in the mutual diffraction volume of the two objective lenses affect the light getting through the pinhole. Here two 'cells' are shown in object space. Images are restricted by the illumination and by the pinhole in image space.

An object that is not in the focal volume may not be illuminated at all. Even if the object is in the illumination beam but out of the focal plane, most of the light it remits misses the pinhole and thus does not reduce the contrast (cell 2 in figure 14). So only an object in the volume confocal to the source and pinhole will contribute to the detected light. This is really all there is to confocal microscopy—the rest is engineering detail.

A single illuminated point is not very useful, so some of the detail involves how to accomplish the scanning. The dimensions of the confocal volume are the microscope resolution, and that detail is pretty important to microscopists.

1.4.1. Confocal resolution. The confocal volume schematized in figure 14 defines the resolution of the confocal microscope. We already know that the illumination of that volume is described by equation (A9) and figure 6. The same three-dimensional point-spread function describes the observation volume, so the volume both illuminated and observed is simply the product of two functions $p(\zeta, \rho)$. If identical optics are used for illumination and observation, this becomes

$$p_{\text{conf}}(\zeta, \rho) = p(\zeta, \rho) \times p(\zeta, \rho), \tag{20}$$

which is shown in figure 15.

Equation (20) is one we will refer to repeatedly, so it is worth thinking about its origin. I think of $p(\zeta, \rho)$ as a *probability* that photons will reach the point ζ, ρ or that photons will be received from that point. Then $p_{\text{conf}}(\zeta, \rho)$ is the product of independent probabilities. The

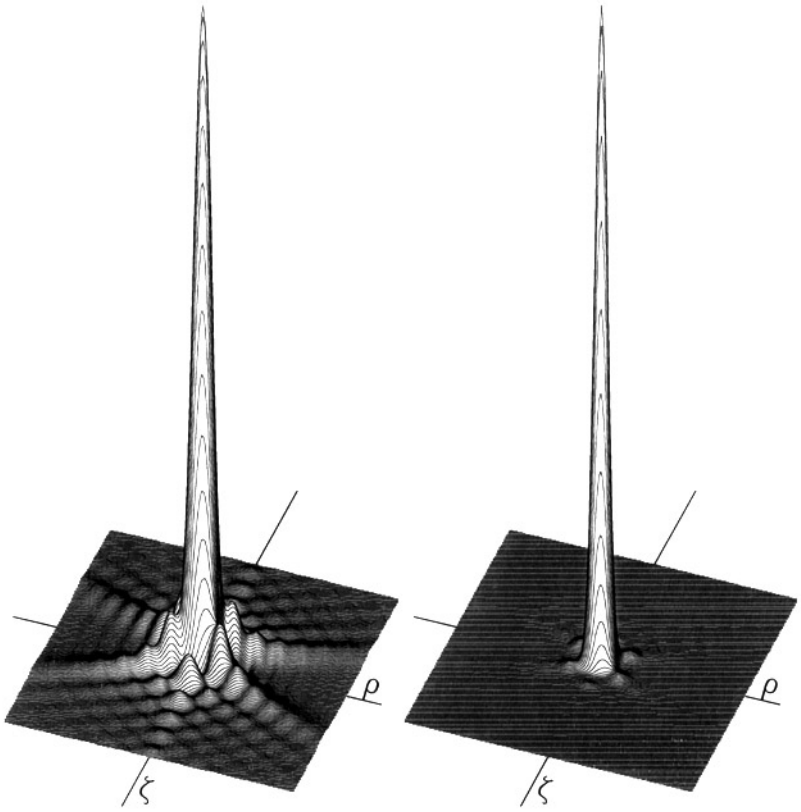

Figure 15. The function $p_{\text{conf}}(\zeta, \rho) = p(\zeta, \rho) \times p(\zeta, \rho)$ for the confocal case is shown on the right. The left is a repeat of $p(\zeta, \rho)$, as shown in figure 6. Again we plot the function over the ranges $\zeta = \pm 24\pi$ and $\rho = \pm 7\pi$, 6 resels in each direction.

function $p(\zeta, \rho)$ occurs when a point source illuminates an objective lens, so later, when the illumination or detection uses a finite pinhole, that will require a convolution of the pinhole and $p(\zeta, \rho)$. Appendix B shows that such a procedure is equivalent to convolving the two functions and then multiplying by the pinhole(s). Remember also that $p(\zeta, \rho) = |a(\zeta, \rho)|^2$, so p_{conf} is a product of four amplitude functions. In appendix C the presence of an object is included, and a phase object requires attention to the $a(\zeta, \rho)$ form.

The resolution limit derived from the expression of equation (20) differs from that of equation (8), because $p_{\text{conf}}(\zeta, \rho)$ is a sharper-peaked function than $p(\zeta, \rho)$, as seen in figure 8(*b*). To obtain the same 26% dip between adjacent peaks, the separation is

$$\Delta r_{\text{conf}} = 0.72 \text{ resel} = 0.44\lambda/n \sin \vartheta, \tag{21}$$

which is

$$\boxed{\Delta r_{\text{conf}} = 0.88\lambda' f/\#} \tag{22}$$

in the notation I remember best, with $\lambda' = \lambda/n$ at the object.

While the confocal resolution is slightly better than the wide field resolution, the dramatic difference seen in figure 8 has more to do with the subsidiary peaks of the diffraction pattern. Like an antenna with suppressed side lobes, the confocal diffraction pattern has much less energy outside the central peak than does the single lens pattern.

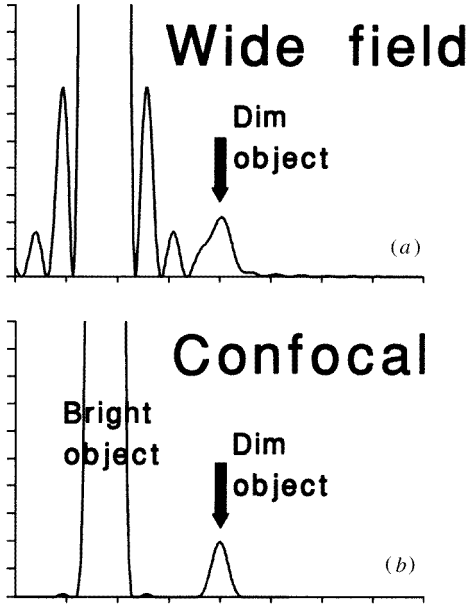

Figure 16. Two points of very different (200:1) remission intensity, are well resolved (4.5 resels). In (*a*) the conventional view leaves the dimmer point obscured, but in (*b*) the confocal contrast enhancement allows its display. Arrows indicate the weaker remitter.

So a bright object near a dim one is less likely to contribute background light—to spoil the contrast. In turn, that means that the resolved dim object can be seen as resolved. As an example, figure 16 shows two point objects in the focal plane that are separated by 4.5 resels and differ in brightness (that is, in remission efficiency) by 200. When the diffraction pattern centres on the dim object, for a conventional microscope the dim object is still obscured by the bright one, but in the confocal case both of the resolved points are visible [13].

Another important difference between $p_{\mathrm{conf}}(\zeta, \rho)$ and $p(\zeta, \rho)$ is that integrals over the parallel planes (ζ= constant) of $p_{\mathrm{conf}}(\zeta, \rho)$ are not equal. In $p(\zeta, \rho)$ every plane parallel to the focal plane is crossed by the same amount of energy, but in the confocal case the function $p_{\mathrm{conf}}(\zeta, \rho)$ does not represent an energy at the plane, it describes energy that has reached the plane and then passed the confocal stop—the pinhole. The integral over planes of constant ζ for $p_{\mathrm{conf}}(\zeta, \rho)$ falls to zero with a half-width of about $\zeta = 0.6$: $\int p(0.6, \rho)\rho \, \mathrm{d}\rho \approx \frac{1}{2}$. Thus planes parallel to the focal plane, but more than $\zeta = 0.6$ away from the focus, do not contribute obscuring light to the image. These matters have been discussed in greater detail by a number of authors [7, 12, 14] .

The consequence, then, of confocal detection is that the resolution is less degraded by variations in contrast, and that resolution is slightly improved. The dramatic difference appears when we extend this analysis out of the focal plane.

1.4.2. Axial resolution. The contrast enhancement that discriminates against nearby scatterers in the focal plane becomes dramatic when the obscuring objects are out of that plane. In figure 8(*b*) there are almost no intensity peaks out of the focal plane. Along the optic axis equations (20) and (A9) reduce to $\left(\sin\frac{\zeta}{4}/\frac{\zeta}{4}\right)^4$. Again Rayleigh's 26% dip will serve to define resolution:

$$\Delta\zeta_{\mathrm{axresel}} = 0.2 \times \pi \cong 0.6, \tag{23}$$

or

$$\Delta z_{\text{axresel}} = 1.5\lambda/n\sin^2\vartheta = 1.5n\lambda/\text{NA}^2, \tag{24}$$

or, in my preferred form,

$$\boxed{\Delta z_{\text{axresel}} = 6\lambda'(f/\#)^2\,.} \tag{25}$$

Unlike a depth of focus criterion, this is truly a resolution. Two equally bright points on the axis separated by $\Delta z_{\text{axresel}}$ are resolved. Further, since the total light reaching the detector from out-of-focus planes also falls off sharply with $\Delta\zeta \cong 0.6$, this axial resolution is really available. From equations (21) and (24) we see that the axial resolution is about the same size as the radial resolution for the confocal case, at least in the realm of microscopy where $\text{NA} \approx 1$.

Confocal microscope designers like to measure the axial resolution by moving a surface through the focal plane and plotting the returned signal as a function of z. They use the full width at half maximum intensity as a figure of merit, but often refer to it as the 'axial resolution'. The full width at half maximum for the function $p_{\text{conf}}(\zeta, 0)$ is related to the resolution of equation (24) by

$$\text{FWHM} = 0.84 \times \Delta z_{\text{axresel}}\,. \tag{26}$$

1.4.3. Pinhole. There are not too many free parameters in confocal microscopy, although there are many ways to implement control of those parameters. One obvious variable is the size of the confocal stop—the pinhole. The bigger the pinhole, the more photons get through it, but also the less discrimination against scattered light from outside the focal volume. The psf is *not* related to the pinhole. Rather, the psf reflects the numerical aperture of the objective lens, while the pinhole's image in the object plane describes the area of that plane from which photons will be collected or to which they go. A pinhole smaller than one resel does not improve resolution, it just loses light. A pinhole 1 resel across allows full use of the objective lens' resolution, but does not actually change the resolution. A pinhole three resels across seems to be a good compromise.

It is convenient to refer all measurements to one plane, so I use the object plane as a reference and scale external objects accordingly. That is, the pinhole might be physically a convenient 1 mm across, but a 100× objective lens reduces that to 10 μm at the object. In that same object plane the 100× objective lens might produce a resel of 0.5 μm. The focal volume then is more specified by the 10 μm circle than by the 0.5 μm resel, as we shall see.

In equation (20) I simply multiplied the two psf's that are detailed in appendix A as equation (A9). But a larger pinhole will smear the psf over the pinhole's image in the object plane—a process that is described by the convolution of the psf and the pinhole. In the limit where the pinhole is very large (compared to a resel), the object plane contains just a slightly blurred image of the pinhole. A typical convolution is shown as $p5(0, \rho)$ in figure 17 (in the focal plane) for a 5 resel pinhole. Now suppose that was the focal volume in the detector channel, and that the source psf comes from a subresel pinhole—as it will for laser illumination. Then the analogue of equation (20) multiplication of two equal psfs is to multiply the convolved psf, $p5(\zeta, \rho)$, by the subresel psf(ζ, ρ), to give the confocal acceptance function labelled $p5(0, \rho) \times \text{psf}(0, \rho)$, in figure 17. The delightful result here is that the confocal effects are pretty well preserved—both lateral and axial resolutions are close to those of equation (20) and figure 8. It is only when both source and detector pinholes are large that the situation degrades toward the wide-field limit.

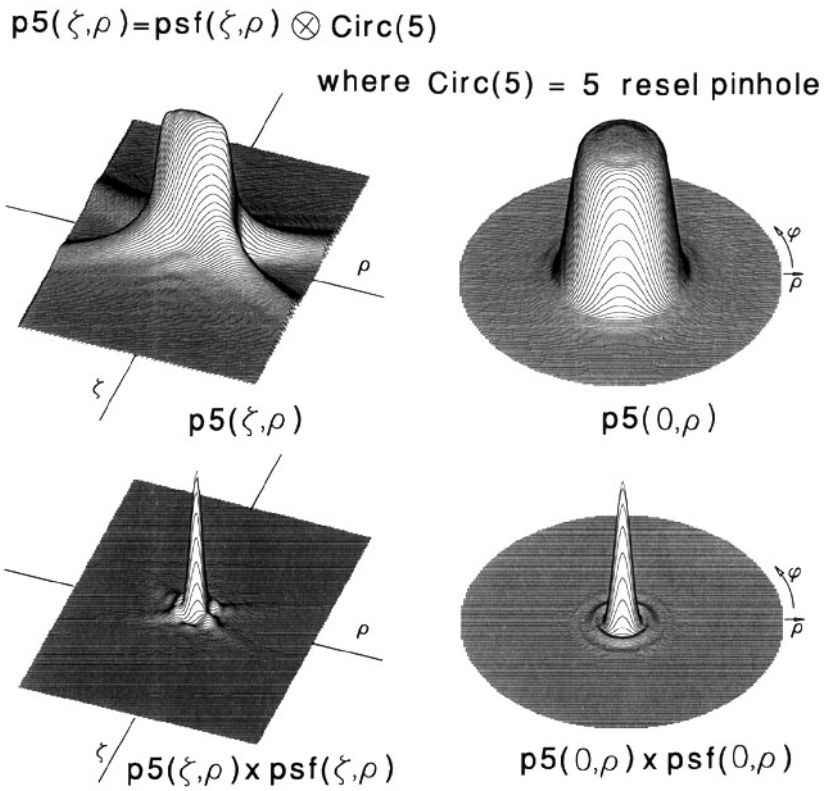

Figure 17. Point-spread functions for a 5 resel pinhole. In the upper views the function $p5$ might describe the detection volume for an objective lens and a pinhole: the psf of the lens is convolved on a 5 resel pinhole. In the lower views $p5$ from the upper views has been multiplied by another psf of the (illumination) lens to give a confocal psf. Left views are in the ρ, ζ plane (ζ is the vertical axis). Right views are the more familiar psf in the $\zeta = 0$ plane. In this display the extent is 10 resels.

A consequence of this result is that the disc scanners that have identical source and detector pinholes must trade off brightness for resolution, while the laser scanning microscopes can use larger collection pinholes without as much of a penalty. The limit of infinite detector pinhole (the detector fills the collection pupil) is still of much higher contrast than a wide-field view, because only the single three-dimensional psf is filled with photons at any instant.

1.4.4. Depth of focus. Depth of focus and axial resolution are not exactly the same thing. Resolution is a well defined term, as described above. Depth of focus is usually given as the axial distance between just-blurred images [15], but the definition of acceptable blur may be a matter of opinion. If the blur is enough to spoil the Rayleigh criterion by doubling the apparent resel size, then the depth of focus turns out to be the same as the axial resolution for a confocal system, which seems wrong. Think, however, of the familiar focusing of a microscope. A thin sheet of cells, say, is in focus, and then $\Delta z = n\lambda/2\mathrm{NA}^2$ away the resolution is spoiled enough so the view is 'out of focus'. But as much as $100\Delta z$ away there is still a blurred image interferring with whatever is in the focal plane at that time.

In the confocal situation, at $3\Delta z$ the background is actually dark—a profoundly different situation.

Confocal microscopists have moved a plane mirror or diffuser through the focus to use the profile of detected intensity as a measure of axial resolution. That measures the total light returned from all scatterers or reflectors in the illuminated region. The detected light is

$$D(\zeta) = \int p(\zeta, \rho)\rho \, \mathrm{d}\rho, \tag{27}$$

which is the quantity whose full width at half maximum (FWHM) is taken as a measure of depth of focus or axial resolution.

2. Implementations

The idea of a confocal microscope is surprisingly easy to implement. In this section I will survey some of the wide variety of realizations of the confocal principle. The main idea, of course, is to move the focused spot over an object, so as to build up an image. Most commonly this will be accomplished sequentially, so that each image element is recorded during a short instant, after which another image element is recorded. The disc scanners are a multiplexed version of this, in which many spatially separate object points are viewed simultaneously, with a neighbouring set of points recorded at a later time. However, the main task in implementing a confocal microscope is to record each of some quarter of a million point images through a confocal optical train. The only real constraint is to keep the detector pinhole confocal to the source point and to its image on the object.

2.1. Stage scanners

The simplest way to achieve confocal imaging is to leave the optics fixed and move the object. There are two major advantages to moving the object: all the lenses work on axis, and the field of view is not constrained by optics. Lenses can easily be diffraction limited for the single on-axis focus. The field of view of optical instruments is seldom more than 1000 resolution elements, with 200 being more typical for microscopes. But if the field is simply one resel, the object can be moved 10 000 times that without change of optical quality. Less urgently, the position of items in the field will be known absolutely, rather than scaled by the optical transfer. Figure 18 shows a typical version of such a stage scanning confocal microscope.

Not surprisingly, early versions of the confocal microscope were stage scanners. This is true of Minsky's microscope [16] and that of Davidovitz and Eggers [17]. One of the confocal microscopes sold commercially by Meridian is based on Brakenhoff's [18] design and is a stage scanner. Perhaps less obvious, all CD players are confocal microscopes with moving objects at least in one direction, and Benschop [19] has designed an imaging version using this technology. One version of the transmission confocal microscope of Dixon [20], which we will discuss later, also uses a moving stage. Much of the exploratory work on confocal microscopy itself has been done on stage scanning microscopes, because of the freedom from complex optics. Only the on-axis (spherical) and chromatic aberrations remain to be corrected in these optics. The primary drawback to this elegantly simple design is that it is slow, and it cannot be made faster. Consider, for instance, a microscope with 250 000 pixels, to be viewed raster fashion with a moving stage in 5 s. Typically, the pixels may be about 1 μm apart, so the stage must move 500 μm from rest to rest in 10 ms.

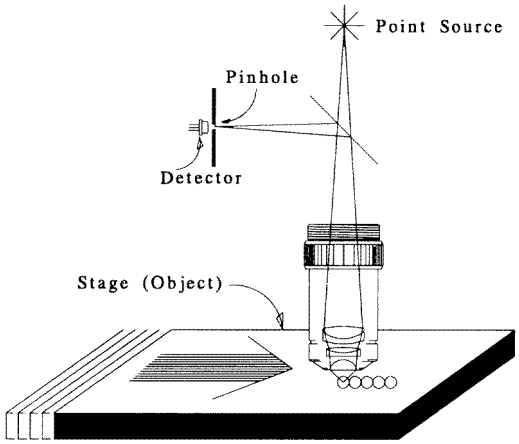

Figure 18. A stage scanning confocal microscope. The objective lens forms a spot at its focus, and the object is moved so that the spot falls sequentially on each of the points to be viewed. A very large image, with absolute position referencing, can be formed, and each resel will be truly diffraction limited, since the optics work only on-axis.

Most conservatively, the motion is sinusoidal and the acceleration is 20 g, not a happy environment for many samples. The acceleration is quadratic in the time, so a 1 s image subjects the sample to 500 g.

2.2. Moving laser-beam scanners

For reasons of speed it makes sense to move the laser beams rather than the object. Most developed confocal microscopes use this approach, with the beam scanners most typically small mirrors mounted on galvanometer actions. Such an implementation is shown in figure 19. There, two galvanometers move (‘scan’) the laser beam in a raster pattern

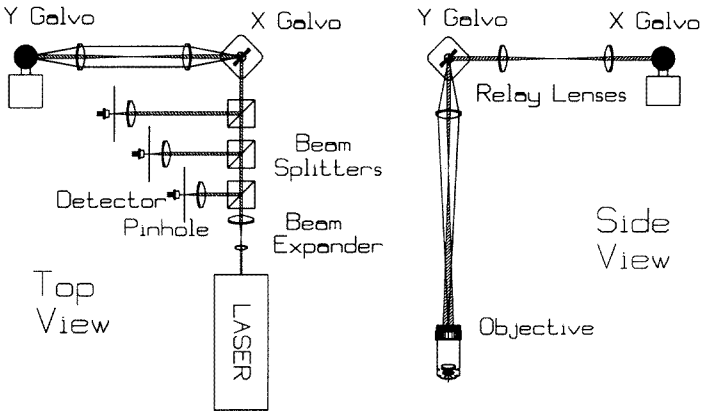

Figure 19. A typical confocal scanning laser microscope using two galvanometers for the beam deflection. The conventions here are the same as in the general microscope figure (figure 3).

like that of a television screen. One direction (traditionally called x or horizontal) is scanned 100 to 1000 times faster than the other (y or vertical). Now, of course, the beam

mostly traverses the optics off-axis and the scanned field is the traditional one allowed by the microscope objective lens. This course of action is possible because many years of development have gone into refining the optical quality of microscope objective lenses. Even so, new objective lenses are being developed specifically for the confocal systems, and it seems likely that these confocal scanning laser microscopes (CSLMs) will remain the dominant ones in biological work for the near future. I will describe many of the features of the CSLMs, but the serious student should avail herself of the wealth of detail in the *Handbook of Biological Confocal Microscopy* [21].

This is the point at which we revisit the basic schematic microscope of figure 3. In order to move the focused spot over the object we must move the laser beam, generally by changing its direction—its angle. A change of position in an object plane is equivalent to a change of angle in an aperture plane, so the moving mirrors need to be in planes conjugate to the pupil (entrance, exit, whatever). This has the advantage that the necessary physical surfaces are not conjugate to the image, so that flaws do not show up as local defects. Figure 19 shows one arrangement, in which both x and y galvanometer mirrors are precisely in aperture planes.

It is a characteristic of the 'beam-scanning' confocal microscopes that the scanning gets done in the pupil planes, by changing angle. The optical design is thus simplified because one can design for the (momentarily) stationary 'beam', and, as a separate calculation, design for the 'scan' [22]. The scan system has pivot points at pupilary planes, where it is simplest to keep the beam collimated. The beam system has foci at the image planes, where the diffraction limit must be tested. It is not my intention to carry out this exercise for the wide variety of confocal microscope designs, but appendix D includes the calculations for one simple CSLM.

2.2.1. Why a laser? Lasers are highly monochromatic and eminently convenient. But are they necessary? The answer is 'usually': the focal spot in a CSLM is diffraction limited, which is to say that its throughput, $\Theta = \Omega a$, is about λ^2, where a is the area of the spot (the Airy disc, say) and Ω is the solid angle subtended by the objective lens at the focus. The radiance theorem [23] requires that throughput be conserved, which means that a fast lens would take light from only a small area of a 1 mm^2 source. For instance, a typical small xenon arc lamp with a radiance of some 80 mW mm^{-2} nm^{-1} in the visible and near infrared might radiate into about 2π sr. The fraction of this power available for a diffraction limited spot is the ratio of λ^2 to 2π mm^2 or about 39 nW in a 10 nm spectral range around 550 nm.

Another way to think of this calculation is by putting the source in the back focal plane of a microscope objective lens. There, a 6 mm pupil 150 mm from the image means $\mathrm{NA}_{\mathrm{back}} = 0.02$, so the resel is 17 μm ($a \approx 225\ \mu\mathrm{m}^2$), and only 0.0002 of the light from the lamp goes into the pupil. So 80 mW mm^{-2} nm^{-1} $\times$ 0.0002 $\times$ 225 $\times$ 10^{-6} mm^2 $\times$ 10 nm $\approx$ 36 nW over a 10 nm bandwidth.

By contrast, a small laser putting 1 mW into its diffraction limited beam will deliver that full mW to the focal spot.

Now we can ask how much is needed, and that is where the 'usually' comes in. My typical confocal microscopes run at video rate, so the pixel time is 100 ns, and 36 nW means only 10 000 photons. If 1% of these are scattered into 2π sr, an objective lens of NA $= 0.9$ will only pick up half of them, so my signal-to-noise ratio cannot be better than $\sqrt{50} = 7$, and that does not allow for losses. On the other hand, a slower microscope might have a pixel time of 40 μs (a 10 s frame rate), and that might make an arc lamp feasible. We will see later that confocal microscopes are often used with fluorescent dyes, where the light economy is even worse, and where 'usually' becomes 'always'.

2.3. Reality

It is not my intent to describe complete confocal microscopes in great detail, but this is a good place to note that confocal optics and a moving resel do not make a microscope. The detector in figure 18 has typically been a photomultiplier tube, so that optics after the pinhole spread the remitted light over a large area. Other variants are avalanche photodiodes (smaller and better for $\lambda > 650$ nm) and, for the multiplexed disc scanners, video cameras. The 'point' source indicated in the figure by a star will most likely be a laser. Then optics must condition the beam so that it looks like a point source and so that it fills the objective lens. The objective lens must be filled enough so the spot is diffraction limited at the objective lens' rated numerical aperture. In practice, that means some overfilling of the objective lens by the Gaussian beam of the laser.

If the microscope is to work in fluorescence, filters will be needed in the detection optics at least. More than one detection channel will allow detection of a variety of colours.

Electronics then amplifies the detected signal, and stores it in some way so that the complete image is accessible. Further, electronics controls the moving stage and relates its position to the pixel location in some memory. Figure 20 shows something of the true complexity of such an instrument—which complexity I intend to ignore for the most part henceforth.

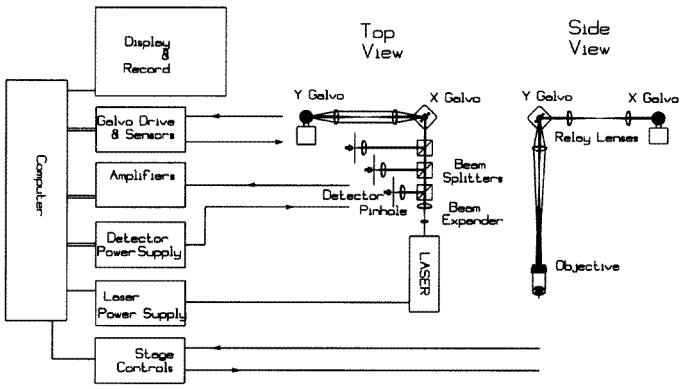

Figure 20. Some of the electrical support needed for a confocal scanning microscope.

2.3.1. Components. The parts of a confocal microscope include the light source, scanners, the objective lens, intermediate optics, the pinhole and the detector, as well as electronic support for many of these. A very complete reference on all of these components is the *Handbook of Biological Confocal Microscopy* [21] (HBCM). I will make some brief comments on each, but I caution that HBCM has whole chapters on each of these topics, and by no means exhausts the subjects.

Lasers. Any laser will do, of course, but some are better. In the visible, argon ion lasers provide CW light at 488 and 514 nm, both useful for chromophores and fluorophores. These lasers have other (weaker) lines in the 275–530 nm range, useful if truly needed. Small argon lasers emit about 5 mW at 488 nm, the strongest wavelength. Large ones can deliver 10 W. The noise [24] on an argon laser is about 1% RMS, usually in the DC to 2 MHz range. Other CW gas lasers are similar, with the various HeNe lasers quieter but less powerful.

The HeCd at 325 nm and 440 nm is noisier and has plasma lines strongly modulated around 2 MHz. Argon lasers are typically the laser of choice for pumping both dye lasers (inconvenient but tunable to any desired wavelength) and some solid state lasers like the Ti:sapphire that is tunable through the near infrared.

Solid state lasers include semiconductor devices and the doped 'glass' lasers, of which Nd:YAG is the most common. Another light source pumps such a laser, and the laser's infrared wavelengths are often doubled into the visible. Noise is less than 0.01% in the semiconductor lasers and not much more for the glass lasers. Beam quality has been a problem for semiconductor lasers, but the new vertical cavity surface emitting lasers (VCSELs) are much better. Poor beam quality makes it impossible to form a diffraction limited spot without throwing away some (much) of the light.

Pulsed lasers have not been used much in confocal microscopy, although they are ubiquitous in biology—usually to pump small dye lasers. The problem is that the pulse repetition rate is generally too low for the sequential pixellation of a confocal microscope. Lots of photons can be packed into one pixel time, but there may be a long wait for the next pixel.

Scanners. The scanning devices that move the laser beams are most commonly moving mirrors. Those mounted on galvanometer actions work well and fill the need for most confocal microscopes. The beam system [22] has an optical invariant, throughput or étendue in two dimensions, the Lagrange invariant in one. Similarly, the scan system has such an invariant: the product of the beam diameter at the mirror (now in a conjugate of the microscope's pupil plane) and the optical scan angle form a conserved quantity. For example, one of the scan pivots is at the objective lens' 6 mm pupil, and the beam sweeps over 18 mm in the plane 150 mm before the pupil. Then the scan angle at the pupil is 0.12 rad and the invariant is 0.7 mm $\times$ rad. That means the galvo with a 10 mm mirror must move the beam through 0.07 rad = 4°. That is easy, even at rates like 200 Hz. Thus a galvo is the device of choice for microscopes that do not need fast frame rates. The frame rate calculation is this: a raster of $h \times v$ pixels takes T s to scan a line of h pixels, and there are v lines, so vT seconds per frame, where $1/T$ is the faster scan frequency. A 500×500 pixel raster with $1/T = 200$ Hz takes 2.5 s. It is not surprising that this is the top speed of most commercial confocal microscopes. Further, the faster frame rates offered are generally for rasters shortened in one dimension only. For instance, one gets 5 frames per second with a raster of 500×40 pixels.

Beamsplitter. Epitaxial illumination means illumination from the observation side, which is the most common arrangement in confocal microscopy. Some kind of beamsplitter separates the illumination and observation beams, and the price is always lost light.

In fluorescence imaging the observation is always by light of a longer wavelength than the illumination. The beamsplitter for fluorescence can then be a dichroic mirror that transmits one of these wavelengths and reflects the other. Ideally the separation is perfect so that all of the illumination light reaches the object and no fluorescence light is lost on the way back to the detector. The two wavelengths are often closer than is comfortable for dichroics, so ideal separation is not likely. If some light must be lost, it is best to keep all the fluorescence possible and lose some illumination. Lost illumination can be replaced by buying a bigger laser—until photobleaching becomes the dominant problem.

Photodestruction by bleaching is a major problem for fluorescence imaging in biological samples. When bleaching occurs, the illumination energy must be kept below the destruction

level, and all other choices depend on that criterion.

Imaging in directly remitted light requires some further loss of light. Most simply, the beamsplitter could be a 50% half-silvered mirror. Then half the illumination light is lost, and half the remitted light. Again, a more powerful laser allows one to choose a 90% mirror: only 10% of the original laser light gets to the object, but 90% of the remitted light reaches the detector (ignoring other losses). Such a division uses light falling on the object efficiently, so light damage can be minimized.

Other devices than partially reflecting mirrors will separate beams. One simple method is to divide the pupil spatially. Clearly if half the pupil is transmitting and the other half receiving, the split is again 50–50. The cost then is in resolution: the full aperture of the objective lens is not available to form the focal spot. However, if the highest resolution is not needed, this is a very clean means of separating the beams. One spatial separation pattern is annular, with the centre of the pupil used for illumination and the outer annulus for collection. Another separator is the fibre coupler. If an optical fibre forms part of the light paths, then a directional coupler can give almost loss-free separation. We will see this later when I discuss the fibre confocal microscopes.

Intermediate optics. The simple diagram of a confocal microscope ignores the reality that some fairly complex optics is required to condition the beams and deliver them to the right places. In figure 19, for instance, the raw laser beam is expanded to fill the objective lens' pupil by a pair of lenses forming an afocal telescope—a beam expander. The scanning devices (here galvo motors) are at conjugates of the pupil, so a pair of relay lenses intervenes. For an infinity-corrected objective lens a tube lens may be needed, and the detection pinhole and detector need to be convenient sizes and locations. All of this is pretty straightforward in the initial design. Then the trick is to reduce the number of surfaces (4% loss per surface if uncoated) and to fold the paths for reasonable packaging.

Objective lens. Confocal microscopes have used standard microscope objective lenses, for which there is 150 years of development experience. Conventional objective lenses are designed to inspect the layer just under a glass cover slip 170 μm thick. Immersion oil, if used, matches the cover slip glass. But for confocal microscopy the observation plane is within a medium of refractive index close to water (1.33), and at a distance between 0 and 2000 μm from the lens. Not surprisingly, a fair number of papers have analysed the consequences of this discrepancy, but water immersion objective lenses specially designed for confocal microscopy are becoming available. All the usual objective lenses for phase contrast, extra flat fields and so forth, are used, but we can expect to see special versions of these too in the future.

Pinhole. The detector pinhole that forms the third confocal conjugate makes confocal microscopy possible. The smaller the pinhole, the better the discrimination *against* scattered light, but also the less light gets through to the detector. Different circumstances require different compromises, so the pinhole may be selectable by the operator. I have used a simple wheel of pinholes in a range of sizes [29]. The wheel approach has also allowed us to use an annular pinhole for discrimination against singly scattered light. One of the early lessons of real confocal microscopes is that tiny pinholes are hard to align, so the physical pinhole should be a lot bigger than its image at the object plane. A resel at the object plane may be 0.2 μm, or 20 μm at 150 mm from the objective lens. It is convenient to magnify that further to 200 μm so that the pinhole need not be difficult to handle and position.

The detector pinhole's position will depend on the actual angle(s) of the beamsplitter, so something must be adjustable. A big pinhole is easy to adjust, but it implies a long optical lever somewhere, so the actual implementation needs care. The pinhole must be at a conjugate of the object plane. However, it is useful to have the detector at a conjugate of the pupil plane so that the detector is filled for all pinhole sizes.

Detector. Detectors for confocal microscopy have been mostly photomultiplier tubes (PMTs). The PMT has the advantage of good sensitivity in the visible, particularly at the blue end of the spectrum, and of least dark noise. Dark noise is like the stray light of section 1.3.2, but it comes from the detector itself. Detector dark noise and amplifier noise are irreducible limiters of the discernible contrast, so it pays to choose detectors and amplifiers that make them small. PMTs are the best detectors in the visible when very few photons are available to be detected, as long as the reason for that scarcity is not speed. When the imaging is at video rates and when the wavelength is beyond 700 nm, a solid state analogue of the PMT works better: the avalanche photodiode (APD) [25]. On the other hand, when there are very few photons, it pays to count them in each pixel. Photon counting techniques can be used with any detector, and are common with PMTs and APDs. For photon counting, the detector circuit threshold is set to give a large response to any excitation by a photon, but to ignore the smaller pulses from internal random events. That effectively reduces dark noise, but requires substantially slower response than direct detection.

The detector in a scanning laser microscope is a single device that converts remitted photons to a voltage stream, reflecting the sequential nature of the beam scanning instruments. When multiple detectors are used—one for each of a few wavelengths—each is of the sequential variety.

Output electronics. The detected signal from a beam-scanning confocal microscope is usually an analogue voltage stream that can be used directly to drive a monitor or CRT. However, storage and display independent of acquisition speed require digitization. The components of the output electronics train thus include analogue-to-digital converters and associated amplifiers and filters to keep the signal from displaying the artefacts of pixellation [11]. These artefacts include loss of resolution (blurring) and aliasing (introduction of Moiré patterns that are not present in the object). None of this is particularly special to confocal microscopy, and the relevant theories were worked out in the early days of telephony. However, it is important to remember that the imaging does not stop at the last optical element. Just as each lens needs to be matched to its neighbours, so each component in the electronics train must be matched in impedance, bandwidth and noise figure.

Control electronics. Electronics controls every moving device in a confocal microscope. This includes the position of the focal spot in three dimensions, the intensity of the illumination beam and the various choices of filters and detection parameters. Most of this is usual for a complex instrument, so I will not dwell on it. The parameters that require special attention are those specifying the position of the spot. Galvanometer motors, the most common beam movers, have feedback signals to tell where they are pointed. In addition, even these simplest of the deflectors are often interrogated by a subsidiary laser beam to determine the local position and linearity of the spot more accurately than with electrical feedback alone. The position in depth of the focal spot can be known relative to some fiducial surface if the moving device (generally the stage) is interrogated by a position

sensor. Because the scale here may be about that of a wavelength, interferometric sensing is appropriate (and easy).

2.4. Image plane scanners

Confocal microscope implementations fall into two major groups, and this is the second. Here the scanning is not done by changing the angle of a single beam at a pupil plane, but rather by changing the position of the source and detection conjugate points in an image plane. Since the intention is to move the confocal point over the object, it is conceptually more direct actually to move the conjugate points. An obvious drawback is that it is hard to get much light through a moving pinhole. This difficulty is solved by using many (2500, say) pinholes simultaneously, by using a slit and sacrificing confocality in one dimension, or by using more than one source and lighting them sequentially. An advantage of the image plane scanners is that normal integrating detectors (eyes and video cameras) can be used to record the image. Also, the multiplex advantage of many simultaneous confocal points allows use of non-laser sources.

2.4.1. Moving pinhole scanning. The simplest way to move a light source and detection pinhole in an image plane is to do exactly that: a physical pinhole in an image plane passes light for the illumination and the same pinhole or a paired one passes the remitted light for detection. Then the pinhole moves over the image plane, from pixel to pixel until all pixels have been visited.

The Nipkow disc. An early television scheme was that of Nipkow, in which a disc with many holes was rotated in an image plane. The holes cover about 1% of the image plane space at any instant, and rotation of the disc maps out all of the required pixels. These modern versions follow Nipkow's arrangement of the pinholes along Archimedes' spirals.

Petrán's tandem scanner. Petrán [26] first used a Nipkow disc to implement a confocal microscope, shown in figure 21. He called this a 'tandem scanning microscope' because the illumination came through one side of the disc and the detection followed in tandem

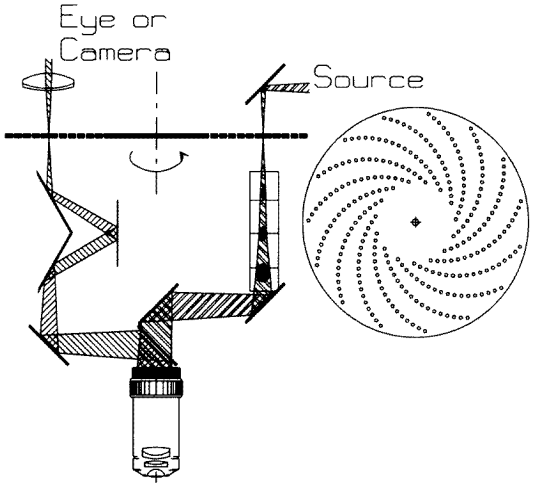

Figure 21. The tandem scanning microscope of Petran. The dove mirrors are needed to match pairs of pinholes across the disc. The source may be an arc lamp, and the image is viewed in real time by a camera or the eye.

through the other side, which must be exactly matched, hole for hole. Petran's original work used the sun as an illumination source, transferred in from a heliostat! Not only is it important that the holes be matched pairwise across the disc, but the alignment requires an image inversion and no distortions over the image of the field at the disc. Not surprisingly, tandem scanning microscopes tend to show some artefact lines due to these difficulties. Intermediate optics become important in these instruments, and the requirements for the objective lenses are stringent—but no more so than for wide-field microscopes.

The great advantage of the tandem scanning approach, however, is that the disc and pinholes of the illumination train are not visible to the detection optics. Only the light that actually gets through the illumination pinholes needs to be dealt with.

Kino's single-sided disc. Kino's modification of the tandem scanning arrangement [27] is to use the same pinholes for illumination and detection. That makes alignment automatic and relaxes the requirement on the intermediate optics. Figure 22 shows how the single-sided disc copes with reflections from the disc surface and the pinhole edges. First, the disc is made of reflecting material (black chrome 1 μm) plated onto a transparent substrate, so it has nearly zero thickness, and the surface is optically polished to reduce scattered light. The holes are made using lithographic techniques. The light specularly reflected from the disc is kept out of the detection channel by tilting the disc so that the (well defined) ghost image is dumped harmlessly. The pinholes have no thickness, since they are simple holes in the plating, but anything conjugate to the image may be seen, so crossed polarizers reduce any scattering from their edges. We expect light remitted from the object to be depolarized, so the polarization wastes half of it—but (one hopes) all of the direct scatter from the pinholes is rejected. The single-sided disc microscope has been used extensively in viewing semiconductors, where light economy is not such a problem as in biology.

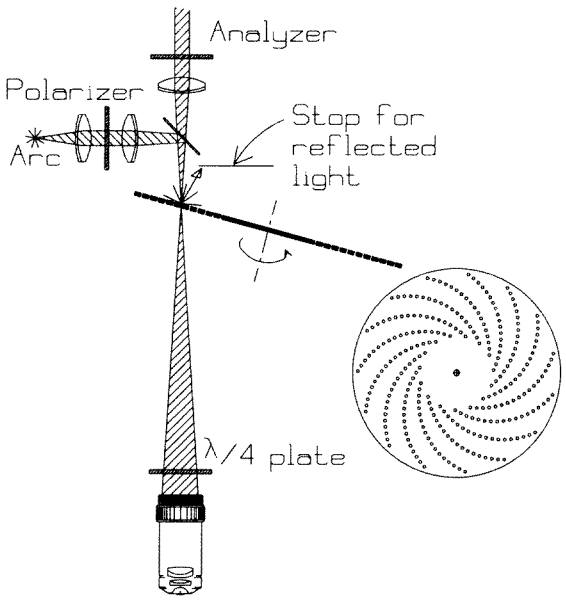

Figure 22. Kino's variant on the TSM solves the alignment problem by using the same pinhole(s) for illumination and detection. The disc is tilted so that reflections from it can be blocked. Polarizers control further scatter from the pinholes.

The oscillating slit. A variant on the disc microscopes is the oscillating slit device of Lichtman [28]. Here the confocal aperture is a slit that is moved in an image plane and

adapted to work with existing microscopes. Lichtman's design has been developed into a commercial instrument by Wong, and this is sold by Newport Instruments. A single slit in the field reduces the light greatly, and the slit is not a pinhole, so this design has made serious compromises. The gain is a simple instrument that is truly an add-on to a standard microscope, at (relatively) little cost.

2.5. Other scanners

2.5.1. Video rate confocal laser microscopes. Real-time imaging is important in many situations, most obviously for microscopy of living beings and for following fast (bio)chemical reactions. The disc scanners (above) are all capable of video rate imaging, and a number of new approaches have begun to appear. Some of those are included in the sections following this. However, the extension to real time of a laser beam scanning microscope has been known for some time, and depends simply on devices that change the angle of the laser beams fast enough to follow the video standard. That standard specifies 40 ms (US: 33 ms) per frame and 63 μs per horizontal line. Only 50 μs of the horizontal line is displayed, so a 500 pixel line has a 100 ns pixel time.

The scanning laser ophthalmoscope (SLO) is a video rate confocal microscope [29] for imaging the retina of a living eye. It is used clinically and in ophthalmological research to observe both the morphology and function of patients' retinas. In developing the SLO I tried most of the variants for fast scanning. In its final version the SLO uses a spinning polygonal mirror as the horizontal beam deflector. The polygon rotates at 40 000 rpm and has 25 facets. Because of the large rotating mass, the polygon frequency, though crystal controlled, is not stable to better than 10^{-6} so we make it the master 'clock' for the microscope. Each polygon facet is slightly different and thus each horizontal line may be slightly different in brightness or position. Even minute image variations like these are quite visible to the human visual system, but they can be made to appear stationary by choosing the number of facets so that it divides integrally into the total number of horizontal lines. With 25 facets in 525 or 625 line television formats, the picture variations are not a bother. A 24 facet polygon produces a 'waterfall' of drifting picture flaws, however.

Another SLO realization used an acousto-optic deflector [22] for the fast scan. This solid state device is fast, quiet, and follows the programmed frequency exactly. A software solution to the inherent chromaticity (the element is diffractive) [30] makes the acousto-optic deflector more attractive. Still, the low transmissivity ($\sim$ 20%) makes it a difficult element for the detection path and newer implementations simply do not bother with full confocality [31]. The slit is nearly as good as the pinhole as a confocal element [32], and this is one of the places where that compromise is made. A difficulty with the acousto-optic deflector is its long narrow pupil, which requires anamorphic optical elements on either side.

Tsien [33] has built a video rate confocal microscope using a resonant galvanometer. Galvanometers should yield higher scan throughput (mirror diameter x scan angle) than polygons, but at 8 KHz they must be resonant—which is to say, sinusoidal in time. Tsien linearizes the sinusoid in time by sampling the signal according to a sinusoidal clock derived from a reflection off the galvo mirror that passes through a coarse grating (a picket fence). The resolution requirement on the clocking circuit is comparable to that on the microscope itself.

2.5.2. Multisided mirrors. The beam scanning confocal microscope encodes spatial information temporally. That is, *where* the flying spot is on the object corresponds to *when*

it is there. This temporal encoding is the reason CSLM detectors need to be non-integrating (PMTs instead of CCDs). However, if the beam to the detector is scanned yet again, it can be spread over a new image space and detected by conventional imaging devices. Although I am not aware of anyone doing this in both dimensions, it works well for one of the scan dimensions.

Koester's three-sided slit scanner. Koester's 'specular microscope' was designed to image the endothelial cells that line the inner surface of the human cornea [34]. There are brighter remissions from the front of the cornea and from the iris that interfere with viewing those cells. Koester achieves sufficient optical sectioning by a one-dimensional scan. Figure 24 shows how one facet of a polygonal mirror is used to scan the image of a slit over the

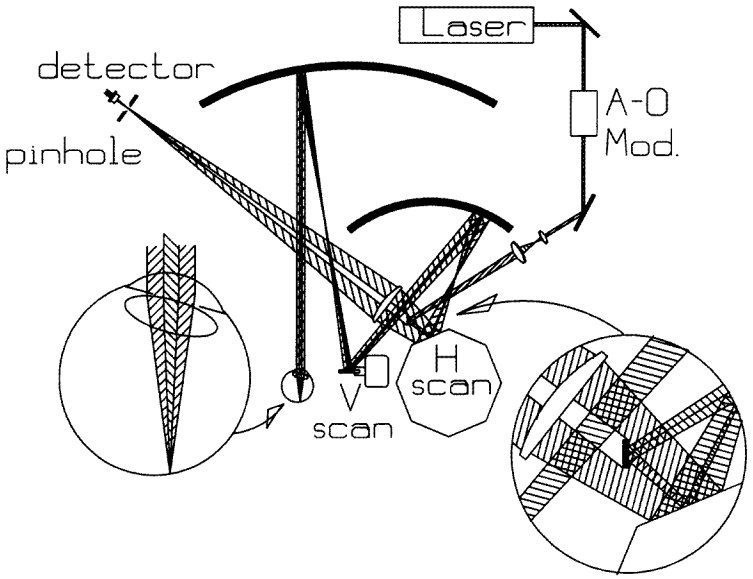

Figure 23. The scanning laser ophthalmoscope (SLO) is a confocal microscope whose objective lens is the lens and cornea of the eye, and whose object is the retina. Human physiology requires specializations of scale, and living subjects need real-time viewing, so this is a video imager.

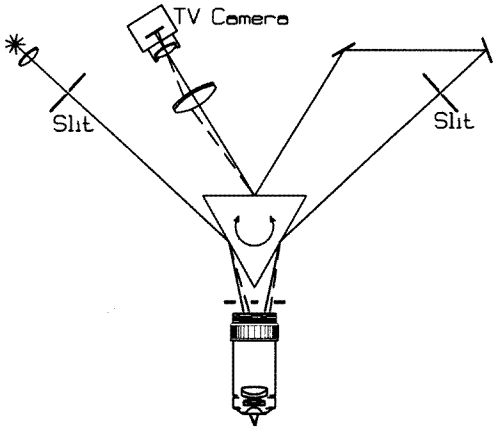

Figure 24. This microscope uses separate pupils for illumination and detection. A slit is imaged on the object and moved over it. Remitted light is descanned by a second side of the oscillating mirror and passes the second slit. The image of the second slit is, in turn, swept over a TV camera or retina to form a viewable image in real time. The slit limits scattered light in the usual confocal way, but is much larger than a resel even in its short dimension.

object. The remitted light is then descanned by another facet of the mirror, and it falls on a second slit in a confocal plane. Now the light falls on yet a third facet that rescans it over an imaging detector like a CCD camera or the human eye. There are some advantages to this confocal microscope beyond the obvious convenience of using an imaging detector. First, the mirror need not move particularly fast, since it corresponds to the slow scan direction of a CLSM. Second, the illumination and detection paths need not overlap in the objective lens's pupil, so that an extra element of discrimination against scattered light is possible, and no beamsplitter is used. For fluorescence detection, a consequence is that fluorescence of the lens never shows up in the detection path. Finally, it is trivial to make this design work at video rates.

Koester and other workers have shown that a design like this that is confocal only in one dimension can approach the contrast enhancement of the CLSM that is confocal in two directions.

Brakenhof's two-sided slit scanner. Brakenhof's [35] variant is to scan a slit image over the sample, descan it with the same mirror onto a confocal slit, and then to use the other side of that mirror to rescan the remitted light over an imaging detector.

2.5.3. Image dissector microscope. A CLSM that comes close to having a flying spot and a flying pinhole has been implemented by Goldstein in a design that has 'no moving parts' [36]. The laser beam is deflected by two acousto-optic deflectors, which produce a lovely clean raster that can work at video rates. The remitted light is detected by an image dissector tube that works like a non-integrating vidicon. The image of the raster falls on the photocathode of this tube, and an electron lens focuses its image in the plane of an electron aperture. Deflecting plates then shift the electron beam so that electrons from the image get through the 'pinhole' synchronously with the optical illumination of the object.

2.5.4. Microlaser microscope. My own latest effort is an all solid state device called the microlaser microscope [37]. The source is an array of vertical cavity surface emitting lasers, which can be packed so that there are one quarter million lasers in a square millimetre. The array is imaged onto the object and one or more lasers are 'lit' at a time. Most simply, a single laser is on for 100 ns, then its neighbour, and so forth, until the whole array has been scanned. From the object's view that looks identical to the flying spot of a beam scanning CLSM. If one laser in 100 is lit at once, this looks more like the tandem scanning situation, but with the brightness of laser illumination.

For detection the microlaser microscope can use an aligned detector array, but more simply it uses the lasers themselves. Remitted light fed back to a laser causes the laser to brighten, and that brighter light is a measure of the remission. A change in the drive voltage is a measure of this feedback, but we use the amount of light itself as the signal. One avalanche photodiode views the whole array, and it should be possible to end up with a fully confocal laser scanning microscope working at video rates and no more than a few millimetres in extent. I hope eventually to use the other ends of the lasers for detection, but at present a beamsplitter is necessary. With a course array of APDs we can expect to multiplex the microlaser microscope to achieve some of the advantages of the disc scanners, but with lasers.

2.6. Variants

2.6.1. Two-photon 'confocal' microscope. Earlier the single-pinhole point-spread function gave way to the confocal psf by multiplication. If the multiplication is not of a source psf times a detector psf, but rather of two source psfs, then the form is mathematically identical. Watt Webb has designed a confocal microscope that uses this idea [38]. Two red photons act simultaneously to stimulate fluorescence that would normally require a single photon in the ultraviolet. Each red photon has an independent probability of being at the object point, and these probabilities multiply to give a confocal psf. The trick, of course, is to get the two photons there at the same time, which requires a powerful source. But the description of the device as a confocal microscope is simple, and verified in Webb's implementation.

Webb and his collaborators use a pulsed laser with a 10^{-5} duty cycle to achieve the proper temporal and spatial crowding. This microscope has the full confocal advantage, as well as an extra consequence of the confocal psf: only at the confocal focus is the photon density high enough for the sample to absorb in the two-photon transition. Thus, unlike a single-photon excitation beam, this flux does no destructive photobleaching of the sample away from the focus. Further, of course, no UV optics are needed.

2.6.2. Heterodyne confocal microscope. Another way to enlist two photons in the imaging

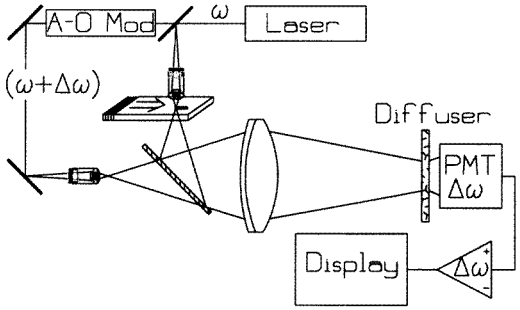

Figure 25. Sawatari's heterodyne microscope.

process is to use interference. Sawatari built a scanning laser microscope using heterodyne detection [39].

Here the remitted photons combine with a part of the original laser beam to form fringes that are modulated by the object's absorption. The double psf is selected, not by a detector pinhole but by the interference condition that requires the remitted photon to traverse a path just as restrictive as that to a pinhole.

More recently, a number of heterodyne microscopes improve on Sawatari's. I like Kempe's [40] microscope because it includes almost everything, and it avoids Sawatari's alignment problems. Figure 26 incorporates much of Kempe's design.

Heterodyne detection. Heterodyne detection is used extensively in radio, radar, holography and wherever small signals can be coherent with a stronger 'local oscillator'. Suppose a signal amplitude A is small compared to various detector artefacts D such as dark noise and amplifier noise, but that a reference amplitude R can be much bigger than those noise components. Then we may mix the two waves to create $A+R$, and detect that. All detectors of electromagnetic radiation are square-law detectors: their output is proportional to the

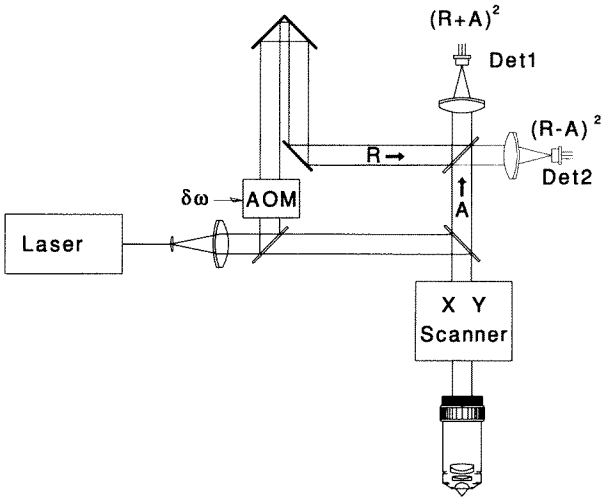

Figure 26. The heterodyne microscope is confocal even without a pinhole at the detector because only photons from the focal volume meet the interference condition. Either detector is sufficient, but together they compensate laser fluctuations. The AOM shifts the reference beam frequency by $\delta\omega$, usually about $2\pi \times 40$ MHz. Additional ζ axis sectioning is provided by giving the laser a short coherence length—such as by using short pulses.

square of the wave amplitude. So detecting A alone we get $S = A^2$, and noise $= \sqrt{A^2 + D^2}$, so for large D

$$\text{SNR} = A^2/D\,. \tag{28}$$

Now if we detect $A + R$, the signal is $I = (A + R)^2 = A^2 + 2AR + R^2 \cong 2AR + R^2$, and the noise is Noise $= \sqrt{A^2 + R^2 + D^2} \cong R$. Since R is a constant, we need only sort out the varying part of the detected wave to get the desired signal. Homodyne detection relies on the variability of A to sort the information from the reference. Holograms use that scheme. However, if A and R have slightly different wavelengths, the desired information will ride on a carrier at the beat frequency:

$$I = (A\cos((\omega + \delta\omega)t) + R\cos(\omega t))^2 \tag{29}$$

$$= AR\,[\cos\delta\omega t + \cos(2\omega t + \delta\omega t)] + R^2\cos^2(\omega t) + \mathcal{O}(A^2)\,. \tag{30}$$

Averaging over times short compared to $1/\delta\omega$, $\langle\cos(\omega t + \phi)\rangle = 0$, $\langle\cos^2(\omega t + \phi)\rangle = \frac{1}{2}$

$$I = AR\cos\delta\omega t + \text{constant}\,. \tag{31}$$

Then a bandpass filter in the electronics at $\delta\omega$ separates out the desired signal: $I_{\delta\omega} = AR$, and the signal-to-noise ratio is

$$\text{SNR} = A, \tag{32}$$

which is the photon-limited value enjoyed by signals robust enough to be larger than the noise artefacts contained in D.

What this detection scheme has accomplished is to increase the SNR from A^2/D to A, but the price is that we need a reference coherent to the signal.

The interferometer in figure 26 provides that coherent reference. The reference beam (the local oscillator in RF terms) is derived from the same laser as the illumination beam, so it is coherent as long as the optical paths are nearly equal. 'Nearly' means within the coherence length of the source.

An extra way to select a narrow range of ζ positions is to use a short coherence length, so that most of the light does not meet the interference conditions. White light has a coherence length of about 50 nm around the 'white light condition', and the superluminescent diodes used in low coherence interferometry [41] have typically 20 μm coherence lengths. Short

coherence lengths also result from short pulses. Kempe's laser delivers 60 fs pulses, so its coherence length is about a pulse length, or 18 μm.

Suppose I add a pinhole at the detector: this now looks like our familiar confocal microscope, with heterodyne detection. But I do not really need to do that because the requirement of interferometric matching is equivalent to a pinhole. Think about our two psfs in the confocal microscope: each is the result of a plane wave or a pure spherical wave falling on the pupil of the objective lens. The function of the pinhole is to ensure that the spherical wave is pure—from a subresolution point. In the interferometer the waves are pure plane or spherical to the extent that they can interfere. A mismatch will result in the detector seeing both a light and a dark fringe, so that the average signal does not change, and that signal is ignored. Thus the heterodyne microscope has the same product of psfs that the pinhole confocal microscope has.

The microscope of figure 26 produces the reference frequency shift with an acousto-optic modulator [42] in a Mach–Zender configuration, but another typical design is a Michelson interferometer with its reference mirror moving for a Doppler shift. In low coherence interferometry that is often a means for scanning the ζ direction, since the white light condition will be met at each ζ in the scan (within the psf). A typical $\delta\omega$ is $2\pi \times 40$ MHz.

The second detector in figure 26 reduces the noise yet further. Detector 2 sees a bright fringe wherever detector 1 sees a dark one. Then (detector 2 $-$ detector 1) drops the constant term and doubles the signal term in equation (31). This compensates for noise such as laser power fluctuations, that are the same in both channels.

Kempe's implementation of the heterodyne microscope includes the possibility of time gating: photons that are delayed due to multiple scattering can be gated out at the detector. That is equivalent to the short coherence length discrimination. Addition of pinholes at the detectors constitute the same sort of overspecification.

An additional bit of information becomes available with heterodyne detection. The two psfs are those of the two objective lenses, but now the phase matters, so all the discussion of the confocal condition should be redone with amplitude psfs. Equation (29) for the intensity at the detector should use amplitude psfs, a complex object, and a final squaring of the combined function at the (square-law) detector. I will not do that, but it should be apparent that phase objects may be imaged—probably best in a transmission version.

2.6.3. Interference confocal microscopes. There are simpler ways to keep track of phase, and microscopes have done that for a long time. Not surprisingly, interference techniques work as well with confocal microscopes as with wide field ones.

Phase contrast. Phase contrast microscopy allows visualization of the variations of refractive index in a transparent sample. A $\lambda/4$ retarder plate in the centre of the pupil shifts the phase of unscattered light relative to that of the light scattered only by small transparent objects, which have been shifted by $-\lambda/4$. The net $\lambda/2$ shift makes these objects seem dark. The retarder also attenuates the much stronger unscattered light. This certainly works in transmission systems [43], but I am not aware of its being implemented in reflection.

DIC. Differential interference contrast uses a shearing interferometer to encode closely adjacent object points. When the second shearing plate recombines the two beams, one may have a slightly different phase from the other. The resulting interference gives changes in refractive index the appearance of casting shadows (in the direction of shear). This is

carried out in the pupil plane, so it is easy to implement in a confocal system, but the returned light must be intense enough to make it useful. Kino has shown this to work in measuring semiconductors, where the application might be termed profilometry, on a microscopic scale [44]. Other differential strategies are possible, and Wilson has demonstrated a very nice one [45] using two modes of a coherent fibre—a technique only possible with scanning laser confocal microscopes.

Mirau interferometer. The reference path in the Mirau interferometer consists of reflection from a beamsplitter half way between objective lens and object, and a mirror at the centre of the objective lens's last surface. Remitted light from the object traverses a path similar except for the object itself. Kino has shown that this is a useful addition to his disc scanning microscope [46], and it should be similarly useful on a laser scanner. This scheme seems to have all the advantages of Sawatari's arrangement, without the alignment problems or the second objective lens. It is, however, necessary to modify the objective lens used for this, and half the working distance is lost. Figure 27 shows the critical area. The heterodyne advantage is available here, though adjusting the reference intensity relative to the signal may be infelicitous.

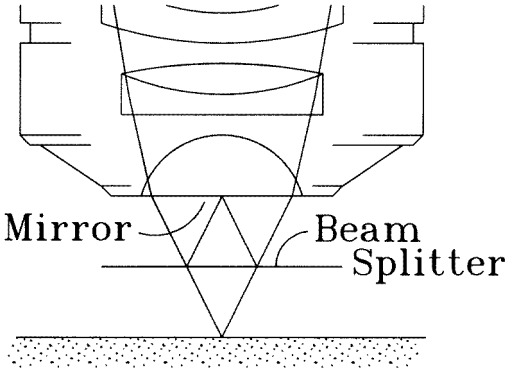

Figure 27. A Mirau interferometer on a microscope objective lens. The beamsplitter directs some of the light back to a mirror conjugate to the object point and then reflects some of that light to the detector. Light reaching the detector from the object has traversed the beamsplitter twice, and interferes with the mirrored reference beam.

2.6.4. Dark field. Dark field microscopy is similar to interference microscopy in that it uses division of the light into two components that emphasize high and low spatial frequencies in the image. However, a simple picture is: the source pupil is an annulus, so that illumination is only at high angles. The detector pupil is an aperture that is the complement of the source pupil. Only light scattered out of the high angles into the low ones reaches the detector, so that the object looks like bright scatterers on a dark field. There is no reason why this idea would not work in the confocal configuration—in reflection or transmission. However, there may be no particular advantage in reflection, where the confocality itself discriminates against unwanted light. In transmission the reduction of the constant background can improve the signal-to-noise ratio significantly.

From the point of view of the point-spread function, dark field works like this: the annular pupil yields a psf that is narrower in the central peak than the full open pupil, but there is substantial energy in the diffraction rings. The smaller central detector pupil yields a broad central peak of the opposite phase (now we have to use the full complex description). The product of the two pupils is zero at the detector unless there has been an object element in the focal volume. The object shifts phase by π for an absorber and by $\pi/2$ for a non-absorbing scatterer. The simple picture really is simpler!

2.6.5. Fibre optic delivery systems. A single-mode optical fibre delivers a diffraction limited beam, so it is a source equivalent to a laser or a subresel pinhole. Not surprisingly, fibres have been used frequently in confocal microscopes [47]. Multimode fibres play the role of larger pinholes, and the various fibre analogues of beamsplitters allow further conversion to fibre confocal microscopes. Oscillating the end of the fibre is equivalent to image-plane scanning, but most implementations use beam scanning. In any case a true microscope objective lens is required since light diverges from the fibre end and must converge to the object.

Appendix A. The point-spread function

In three (scaled) dimensions the amplitude diffraction pattern for intensity taken from Richards and Wolf [6] is found by using an electromagnetic wave falling on a (pin)hole as a source for the field at the point ρ, ζ, φ. Figure A1 shows the axes and the notations. The electric and magnetic field components in the directions ρ, ζ and φ are

$$\boldsymbol{e}(\rho, \zeta, \varphi) = -\mathrm{i}A\,(I_0 + I_2)\cos\varphi\hat{r} - \mathrm{i}A\,(I_0 - I_2)\sin\varphi\hat{j} - 2AI_1\cos\varphi\hat{z} \tag{A1}$$

$$\boldsymbol{h}(\rho, \zeta, \varphi) = -\mathrm{i}A\,(I_0 + I_2)\sin\varphi\hat{r} - \mathrm{i}A\,(I_0 - I_2)\cos\varphi\hat{j} - 2AI_1\sin\varphi\hat{z} \tag{A2}$$

where $\varphi = 0$ is the direction of the source polarization, A is a scaling constant, and

$$I_0(\zeta, \rho) = \int_0^{\vartheta} J_0(\rho\sin\alpha/\sin\vartheta)\sqrt{\cos\alpha}\sin\alpha(1 + \cos\alpha)\,\mathrm{e}^{\mathrm{i}\zeta\cos\alpha/\sin^2\vartheta}\,\mathrm{d}\alpha \tag{A3}$$

$$I_1(\zeta, \rho) = \int_0^{\vartheta} J_1(\rho\sin\alpha/\sin\vartheta)\sqrt{\cos\alpha}\sin^2\alpha\,\mathrm{e}^{\mathrm{i}\zeta\cos\alpha/\sin^2\vartheta}\,\mathrm{d}\alpha \tag{A4}$$

$$I_2(\zeta, \rho) = \int_0^{\vartheta} J_2(\rho\sin\alpha/\sin\vartheta)\sqrt{\cos\alpha}\sin\alpha(1 - \cos\alpha)\,\mathrm{e}^{\mathrm{i}\zeta\cos\alpha/\sin^2\vartheta}\,\mathrm{d}\alpha\,. \tag{A5}$$

Note that $I_1(\zeta, 0) = I_2(\zeta, 0) = 0$. Here $\sin\vartheta = \mathrm{NA}/n$, so from equations (3) and (4), it might be simpler to write

$$I_0(z, r) = \int_0^{\vartheta} J_0(rk'\sin\alpha)\sqrt{\cos\alpha}\sin\alpha(1 + \cos\alpha)\,\mathrm{e}^{\mathrm{i}zk'\cos\alpha}\,\mathrm{d}\alpha \tag{A6}$$

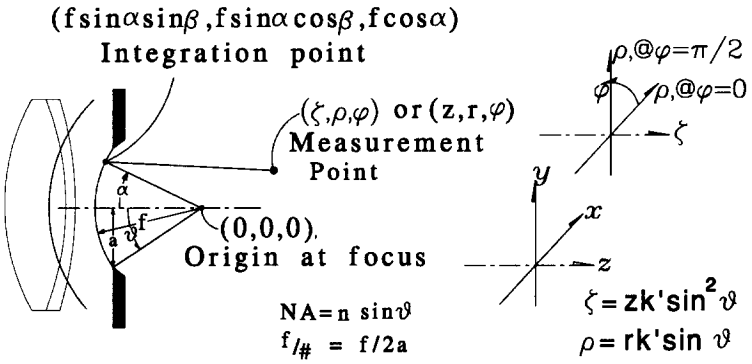

Figure A1. The psf is measured at the point (ζ, ρ, φ) or (z, r, φ) when the focus is at the origin and the integration is carried out over the points of the wavefront in the pupil. It is far from obvious how the above equations follow from this geometry, and the reader is cautioned that [6] is not simple.

$$I_1(z,r) = \int_0^{\vartheta} J_1(rk' \sin\alpha)\sqrt{\cos\alpha}\,\sin^2\alpha\,\mathrm{e}^{\mathrm{i}zk'\cos\alpha}\,\mathrm{d}\alpha \tag{A7}$$

$$I_2(z,r) = \int_0^{\vartheta} J_2(rk' \sin\alpha)\sqrt{\cos\alpha}\,\sin\alpha(1-\cos\alpha)\,\mathrm{e}^{\mathrm{i}zk'\cos\alpha}\,\mathrm{d}\alpha\,. \tag{A8}$$

The point-spread function for intensity is then simply $\boldsymbol{e}\cdot\boldsymbol{e}^* + \boldsymbol{h}\cdot\boldsymbol{h}^*$, for

$$p(\zeta,\rho) = \left\{|I_0|^2 + 2\,|I_1|^2 + |I_2|^2\right\} \tag{A9}$$

where we assume normalization to make various scale factors equal 1. When phase or polarization matter the amplitude psf of equation (A1) must be used.

In the confocal case,

$$p_{\mathrm{conf}}(\zeta,\rho) = \left\{|I_0|^2 + 2|I_1|^2 + |I_2|^2\right\}^2. \tag{A10}$$

This is the confocal point-spread function shown in figures 15 and 8(*b*).

Appendix B. Equivalent convolutions

I like to use the form in which the point-spread functions are multiplied and the pinhole is convolved. This is equivalent to another approach, in which the point-spread functions are convolved and the pinholes are multiplied, as I show in the following schematic:

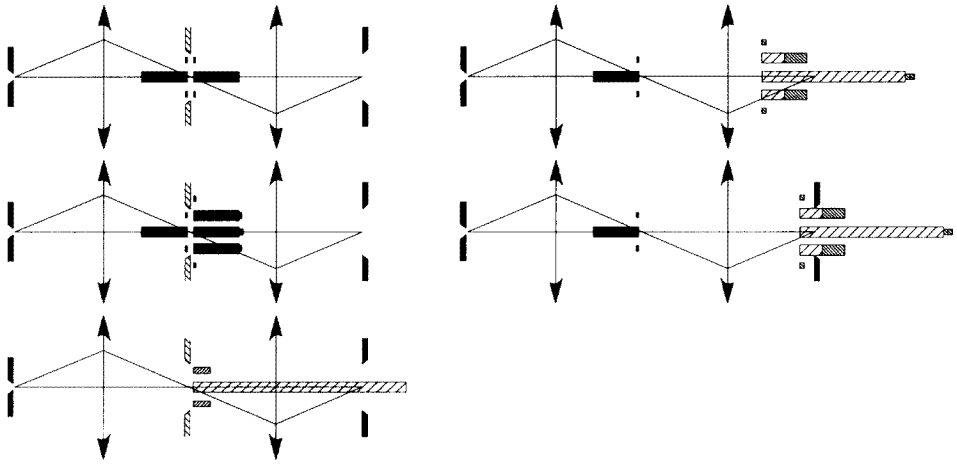

Figure B1. A schematic of the two ways to look at the flow of photons through the microscope. The three left-hand panels illustrate convolution of the detector pinhole on the detector psf, followed by multiplication by the source psf. The right-hand panels show convolution of the source and detector psfs, followed by multiplication by the pinhole. Results are identical.

The left-hand set of panels represents convolution of the detector psf on the detector pinhole. At the left is a pinhole of subresel size, so that the point-spread function in object space is represented by the three bars in ratio 4:100:4 (like the Airy disc). A subresel pinhole to the right would create a psf in object space identical to the one from the left. A finite pinhole (here 3 resels wide) lies to the right and is imaged in object space at unity magnification. First I convolve the object space pinhole on the right psf, to give the pattern of five bars in ratio 4:104:108:104:4, shown in the next left-hand panel. Convolution means summation of the psf in each of the three positions allowed by the pinhole. This is a digitized version of the actual integration implied. Now I multiply the source psf by the

convolved detector psf, to get a pattern of three bars in ratio 416:10 800:416, shown in the third left-hand panel. The intensity reaching the detector through the (real) pinhole is then the sum of these bars: 11 632.

In the second version (right-hand panels) the source psf is again generated, but now each bar of the pattern acts as a subresel source to generate a new psf on the right of the second lens. These three psf copies, scaled by the generating psf, add to give the convolved five-bar pattern in ratio 16:800:10032:800:16 shown in the second right-hand panel. The three-resel pinhole then lets through only the central three of these bars, for a total intensity of 11 632.

This is not magic, it is just an equivalent way of looking at the flow of photons.

In more detail, the calculation is the same:

In the first method, the convolution of the second lens psf $p(\rho, \zeta)$ on the pinhole $D(\rho_D)$ is

$$Q(\rho, \zeta) = \int p(\rho, \rho_D, \zeta) D(\rho_D)\, \mathrm{d}\rho_D, \tag{B1}$$

and its product with the source psf is $Q(\rho, \zeta)p(\rho, \zeta)$, so the photons reaching the detector are

$$D = \int p(\rho, \zeta) Q(\rho, \zeta)\, \mathrm{d}\rho\, \mathrm{d}\zeta = \iint p(\rho, \zeta) p(\rho, \rho_D, \zeta) D(\rho_D)\, \mathrm{d}\rho_D\, \mathrm{d}\rho\, \mathrm{d}\zeta\,. \tag{B2}$$

Here (ρ, ρ', ζ) signifies $(\rho - \rho', \varphi - \varphi', \zeta)$, and $\mathrm{d}\rho = \rho\, \mathrm{d}\rho\, \mathrm{d}\varphi$.

In the second method the two psf's are convolved, $pp(\rho, \zeta) = \int p(\rho, \zeta) p(\rho, \rho, \zeta)\, \mathrm{d}\rho$ then that function is multiplied by the pinhole and all photons are integrated to give

$$D = \int D(\rho, \zeta) pp(\rho, \zeta)\, \mathrm{d}\rho\, \mathrm{d}\zeta = \iint p(\rho, \zeta) p(\rho, \rho, \zeta) D(\rho)\, \mathrm{d}\rho\, \mathrm{d}\rho\, \mathrm{d}\zeta \tag{B3}$$

identically.

Notice that Fourier methods do not help here: the psf's are Fourier transforms of pinholes, so the FT of pD is a similar pair $p'D'$. The reason for this is that although $p(\rho, \zeta)$ is the FT of a hole, the relevant hole is the aperture of the lens, not the source or detector pinhole. So somewhere along the way we need to do a real convolution, and no tricks help.

When both source and detector have finite pinholes (as is the case with the disc scanners), then each contributes a function in object space like that of equation (B1), and the product in object space will be, $P(\rho, \zeta)Q(\rho, \zeta) = (S \otimes p)\,(q \otimes D)$ rather than $p(\rho, \zeta)Q(\rho, \zeta) = p\,(q \otimes D)$. Figure 17 shows the impact of the two finite pinhole situation, and demonstrates that a laser scanning confocal microscope can retain good optical sectioning in high-intensity situations.

Appendix C. The object

I want to return briefly to the point-spread function and view the complete train of optical components, with the final addition of the object itself—the entity my confocal microscope is designed to observe. Following the schematic of figure C1, light from a subresel source pinhole fills the illumination objective lens and appears in the object space as the diffraction pattern $p(\rho, \zeta)$. Since the source pinhole may well be of finite size, the actual pattern in object space is $P = p \otimes S$, where $\otimes$ signifies the convolution operation:

$$P(\rho, \zeta) = p \otimes S \equiv \int p(\rho - \rho_S, \zeta) S(\rho_S, \varphi_S) \rho_S\, \mathrm{d}\varphi_S\, \mathrm{d}\rho_S\,. \tag{C1}$$

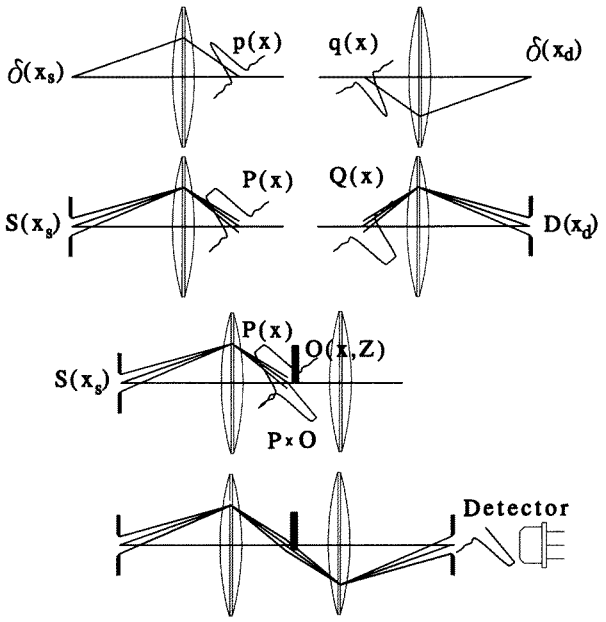

Figure C1. The various point-spread functions that go to make up the image of one object point. The top line shows the psfs of the two objective lenses—or of the single objective lens used for two purposes in epitaxy. The next line includes convolution of the finite source and pinhole. The next line shows the illumination modified by an object, and the last line indicates that the detector accepts the integral of all light from the product of (source function) × (object) × (detection function).

Each point in object space is a source of new wavelets, according to the Huygens principal, but these wavelets may be modified by the presence of the object. The object is some complex function $O(\rho, Z)$ that multiplies, point by point, the distribution $P(\rho, Z)$. Although these psf's are intensity diffraction patterns, there are situations in which the more correct use of amplitude psf's is necessary. I will come back to that.

Now, at the same time that the photons come from the source they are going to the detector, and the right-hand side of the schematic shows this. As I argue in appendix B, this process is equivalent to (anti?) photons coming from the detector to the object space: the diffraction pattern in object space expresses the process equally. Let $D(\rho_D, \varphi_D)$ describe the detector pinhole and $q(\rho, \zeta)$be the diffraction pattern for the detector objective lens. The detector's objective lens is the same as the source objective lens, but I have unfolded the schematic to illustrate. Again the convolution is $Q = q \otimes D$ at the object. So I have two psfs in the same space, each representing the probability that there is a photon there. The joint probability that the photon passes the detector pinhole is then PQ, or POQ if there is an object. What the detector sees is the totality of the photons passing the pinhole, and that will include all the scattered photons from planes other than Z, where I put the object. So

$$\mathrm{Det}(\zeta, Z) = \int \left\{ \int S(\rho_S) p(\rho, \rho_S, \zeta)\, \mathrm{d}\rho_S \right\} O(\rho, Z) \left\{ \int D(\rho_D) q(\rho, \rho_D, \zeta)\, \mathrm{d}\rho_D \right\} \rho\, \mathrm{d}\rho\, \mathrm{d}\varphi, \tag{C2}$$

where the arguments (ρ, ρ') signify $(\rho - \rho', \varphi, \zeta)$. Now I include all the planes of the object space:

$$\mathrm{Det}(Z) = \int \mathrm{Det}(\zeta, Z)\, \mathrm{d}\zeta\ . \tag{C3}$$

That is the intensity of the light at the detector for each location in the scan.

Remember, too, that all of the spatial variables, (ρ, ζ), refer to subresolution divisions. The whole psf is, in a sense, one resel. Therefore, at any instant the subresolution operations described here generate the signal from one resel of the microscope.

Appendix D. Some engineering details

I want to describe a simple confocal microscope in some detail, to give a feel for the kind of attention to engineering detail that is involved. This will be a plain vanilla version of a scanning laser confocal microscope, but I hope to show some of the level of complexity that is involved. I will use the notation of the simple microscope of figure 3, and refer to the detailed figure D1. The objective lens illuminates and observes a psf in plane O, the object plane. At 150 mm from the objective lens is plane O + 1, where the psf is imaged, about 20 μm across, pretty much the same for all magnifications. The next lens in the system forms an image of the objective lens's pupil, which is at plane P, and that image is at plane P + 1. Now P + 1 is the appropriate place to put the scanners, but in fact we need a scanner for each direction and the easiest thing is to put one at P + 1 and the next at P + 2, another image of the pupil.

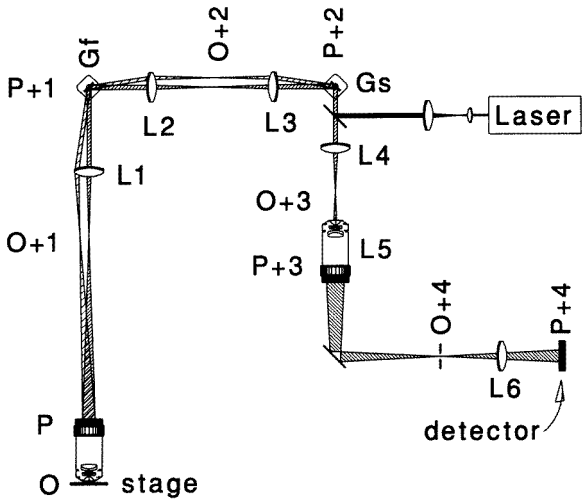

Figure D1. Layout of the detailed confocal microscope. Planes labelled O are conjugate to the object, and those labelled P are conjugate to the pupil. The text explains the details.

That arrangement of scanners is shown in figure 19 for two galvanometer scanners (in this figure the two are shown in the same plane). There are alternatives to the relaying of pupils and there are other possible scanners, but for simplicity these will do.

A maximum usable size for the plane $O+1$ is $20\mu\text{m} \times 1000 = 2$ cm, so lenses can be of reasonable aperture. For simplicity of discussion I will use relay lenses in the arrangement shown, all of focal length 50 mm. In reality I do not insist on collimated beams at the pupil planes or all lenses alike. Now the pupil gets demagnified to P + 1, where it is $\sim$4 mm in diameter, as it will be at P + 2, the second scanner.

After P + 2 the beam is descanned, so we are dealing simply with a 4 mm collimated beam. If the intent is to overfill the pupil(s), then a Gaussian beam must be bigger than 4 mm, but none of this is stressing the speed or size of the lenses.

Next I want a beamsplitter to separate illumination from detection paths. My choice would be a 10:1 neutral beamsplitter, losing 90% of the incident laser light but only 10% of the remitted light. Alternatively, for fluorescence a dichroic beamsplitter lets most of the illumination light through but reflects most of the longer wavelength remission. Other separators use different parts of the area in a plane P + 3 or rely on polarization effects.

The neutral splitter is simplest.

I need a beam expander on the illumination side. Of course, these two lenses can really be included in L1, L2 and L3, but for illustration I show them here explicitly. On the detection side I need to match the resel at O + 3 to a convenient pinhole. I would like to work with a 1 mm resel, but I do not want my microscope to stretch into the next laboratory, so I relay once more to O + 4 and image that on the pinhole with a 40× objective lens. Now the resel at O + 5 is 0.8 mm across and I can chose a nice 3 mm pinhole for my default size, with some larger and smaller ones for variety.

After the pinhole comes the detector, but not immediately. The lens L6 images L5 on the detector, so that the detector is at a pupillary plane (P + 4). Detectors come in various sizes and work best if filled pretty much completely. L6 does that job so that the detector is filled whatever size is chosen for the pinhole.

The position of the psf in three dimensions is controlled by the scanners and the stage. The figure shows both scanners in the same plane, but of course they will have axes orthogonal in reality. Gf is the scanner in the fast (usually horizontal in terms of the display) direction, and Gs scans the slow direction orthogonal to it. The stage controls the axial position of the sample relative to the plane $\zeta = 0$. The settings of all three positioners must be known, so some position detector is part of the microscope. For slow galvanometer actions an electronic feedback system in the drive is often good enough, but more commonly an optical detector is used. I like to use an extra laser beam to find a point on each scan with a split photodiode as detector. More elaborate systems can even follow the nonlinearities of a sinusoidal scan, as long as I am willing to use just as high a resolution in the position sensor as in the microscope. The stage position may be sensed in traditional ways, but counting interference fringes of yet another laser beam appeals to me.

Acknowledgments

This work was supported by DE-FG02-91ER61229 from the Office of Health and Environmental Research of the Department of Energy. The photo of figure 2 was taken by Guy Jirawuthiworavong on a Leitz CSLM in auto fluorescence, excitation at 568 nm. Figure 7, the psf of a real lens, was taken by Juliet A Mervis.

Nomenclature

APD	Avalanche photodiode detector
PMT	Photomultiplier tube detector
CCD	Charge coupled device TV camera—an explicitly pixellated imaging detector
CSLM	Confocal scanning laser microscope
HBCM	[21], *The Handbook of Biological Confocal Microscopy*
pixel	Reference area of display representing one sample of the object (area or volume)
resel	Area (or volume) of the object representing one resolution element of the microscope
SNR	Signal to noise ratio
$f/\#$	f-number: aperture diameter/focal length, $= n/2$ NA
J_n	Bessel function of the first kind, of order n
NA	Numerical aperture, $= n \sin \vartheta$, see figure 4
psf	Point-spread function
$p(\rho, \zeta)$	Point-spread function (intensity: $p = a^* a$)

$a(\rho, \zeta)$	Amplitude point-spread function (includes phase)
n	Index of refraction
λ	Wavelength
ρ	Radial optical unit, equation (4). Born and Wolf's v
ζ	Axial optical unit, equation (3). Born and Wolf's u.

Bibliography

Essential

Pawley J B (ed) 1995 *Handbook of Biological Confocal Microscopy* 2nd edn (New York: Plenum). This is the *sine qua non* in the field. Details of both construction and use are plentifully provided.

General

These are some of the general works on confocal microscopes that will be of use to the student or general user.

Kino G S and Corle T R 1989 Confocal scanning optical microscopy *Phys. Today* **42** 55–62
Pawley 1991 J B Fundamental and practical limits in confocal light microscopy *Scanning* **13** 184–98
Shotton D (ed) 1993 *Electronic Light Microscopy—Techniques in Modern Biomedical Microscopy* (Wiley-Liss) p 351
Slater E M and Slater H S 1993 *Light and Electron Microscopy* (Cambridge: Cambridge University Press)
Stevens J K, Mills L R and Trogadis J (eds) 1993 *Three-Dimensional Confocal Microscopy* (San Diego, CA: Academic)
Webb R H 1991 Confocal microscopes *Opt. Photon. News* **2** 8–13
Wilson T 1985 Scanning optical microscopy *Scanning* **7** 79–87
Wilson T (ed) 1990 *Confocal Microscopy* (London: Academic)
Wilson T and Sheppard C J R 1984 *Theory and Practice of Scanning Optical Microscopy* (London: Academic)

References

[1] Inoué S and Oldenbourg R 1994 Optical instruments: microscopes *Handbook of Optics* 2nd edn, vol 2 ed M Bass (New York: McGraw-Hill) ch 17
[2] Inoué S 1986 *Video Microscopy* (New York: Plenum)
[3] Inoué S and Oldenbourg R 1986 *Video Microscopy* (New York: Plenum) pp 17, 18, they suggest an intermediate image of 28 mm is now possible ($\div 17$ μm $= 1647$ resels), but 18 mm is more common (1058 resels)
[4] Born M and Wolf E 1991 *Principles of Optics* 6th edn (New York: Pergamon)
[5] Hecht E 1987 *Optics* 2nd edn (Reading, MA: Addison-Wesley) p 421
[6] Richards B and Wolf E 1959 Electromagnetic diffraction in optical systems II. Structure of the image field in an aplanatic system *Proc. R. Soc.* A **253** 358–79
[7] Hell S and Stelzer E H K 1992 Fundamental improvement of resolution with a 4Pi-confocal fluorescence microscope using two-photon excitation *Opt. Commun.* **93** 277–82
Van Der Voort H T M and Brakenhoff G J 1990 3D image formation in high-aperture fluorescence confocal microscopy: a numerical analysis *J. Microscopy* **158** 43–54
[8] Sheppard C J R 1988 Aberrations in high aperture conventional and confocal imaging systems *Appl. Opt.* **27** 4782–6
Hell S, Reiner G, Cremer C and Stelzer E H K 1993 Aberrations in confocal fluorescence microscopy induced by mismatches in refractive index *J. Microscopy* **169** 391–405
[9] Lord Rayliegh *Scientific Papers* vol III, p 436
[10] Michelson A A 1927 *Studies in Optics* (Chicago, IL: University Chicago Press)
[11] Webb R H and Dorey C K 1990 The pixelated image *Handbook of Biological Confocal Microscopy* ed J B Pawley (New York: Plenum) pp 41–51
[12] Sandisson D R and Webb W W 1994 Background rejection and signal-to-noise optimization in confocal and alternative fluorescence microscopes *Appl. Opt.* **33** 603–15
[13] Brakenhoff G J, Blom P and Barends P 1979 Confocal scanning light microscopy with high aperture immersion lenses *J. Microscopy* **117** 219–32

[14] Visser T D, Brakenhoff G J and Groen F C A 1991 The one-point fluorescence response in confocal microscopy *Optik* **87** 39–40
[15] Smith W J 1990 *Modern Optical Engineering* 2nd edn (New York: McGraw-Hill) p 145ff
[16] Minsky M 1988 Memoir on inventing the confocal scanning microscope *Scanning* **10** 128–38
[17] Davidovitz P and Egger M D 1969 Scanning laser microscope *Nature* **223** 83
Davidovitz P and Egger M D 1971 Scanning laser microscope for biological investigations *Appl. Opt.* **10** 1615–9
[18] van der Voort H T M *et al* 1985 Design and use of a computer controlled confocal microscope for biological applications *Scanning* **7** 66–78
[19] Benschop J and van Rosmalen G 1991 Confocal compact scanning optical microscope based on compact disc technology *Appl. Opt.* **30** 1179–84
[20] Dixon A E, Damaskinos S and Atkinson M R 1991 Transmission and double-reflection scanning stage confocal microscope *Scanning* **13** 299–306
[21] Pawley J B (ed) 1995 *Handbook of Biological Confocal Microscopy* 2nd edn (New York: Plenum)
[22] Webb R H 1984 Optics for laser rasters *Appl. Opt.* **23** 3680–83
[23] Boyd R W 1983 *Radiometry and the Detection of Optical Radiation* (New York: Wiley). Boyd uses the term étendue for throughput.
[24] Shapiro H M 1987 Laser noise and news *Cytometry* **8** 248–50
[25] Webb R H and Hughes G W 1993 Detectors for scanning video imagers *Appl. Opt.* **32** 6227–35
[26] Petran M and Hadravsky M 1968 Tandem-scanning reflected-light microscope *J. Opt. Soc. Am.* **58** 661–4
Petran M *et al* 1985 The tandem scanning reflected light microscope Part 1: the principle, and its design *Proc. RMS* **20** 125–9
[27] Xiao G Q, Corle T R and Kino G S 1988 Real-time confocal scanning optical microscope *Appl. Phys. Lett.* **53** 716–8
[28] Lichtman J W, Sunderland W J and Wilkinson R S 1989 High-resolution imaging of synaptic structure with a simple confocal microscope *The New Biologist* **1** 75–82
[29] Webb R H, Hughes G W and Delori F C 1987 Confocal scanning laser ophthalmoscope *Appl. Opt.* **26** 1492–9
[30] Kobayashi K *et al* 1991 Confocal scanning laser ophthalmoscope with a slit aperture *Meas. Sci. Technol.* **2** 287–92
[31] Draaijer A and Houpt P M 1988 A standard video-rate confocal laser-scanning reflection and fluorescence microscope *Scanning* **10** 139–45. See also Tsien in HBCM, ch 29.
[32] Koester in HBCM ch 34.
[33] Tsien in HBCM ch 29.
[34] Koester C J, Auran J D, Rosskothen H D, Florakis G J and Tackaberry R B 1993 Clinical microscopy of the cornea utilizing optical sectioning and a high-numerical-aperture objective *J. Opt. Soc. Am.* A **10** 1670–9
[35] Brakenhoff G J and Visscher K 1993 Imaging modes for bilateral confocal scanning microscopy *J. Microscopy* **171** 17–26
[36] Goldstein S R, Hubin T, Rosenthal S and Washburn C 1990 A confocal video-rate laser-beam scanning reflected-light microscope with no moving parts *J. Microscopy* **157** 29–38
[37] Webb R H and Rogomentich F J 1995 Microlaser microscope using self detection for confocality *Opt. Lett.* **20** 533–5
[38] Denk W, Strickler J H and Webb W W 1990 Two-photon laser scanning fluorescence microscopy *Science* **248** 73–6
[39] Sawatari T 1973 Optical heterodyne scanning microscope *Appl. Opt.* **12** 2768–72
[40] Kempe M and Rudolph W 1994 Scanning microscopy through thick layers based on linear correlation *Opt. Lett.* **23** 1919–21
[41] Fercher A F, Hitzenberger C K and Juchem M 1991 Measurement of intraocular optical distances using partially coherent laser light *J. Mod. Opt.* **38** 1327–33
[42] Jacobs S. F 1988 Optical heterodyne (coherent) detection *Am. J. Phys.* **56** 235–45
[43] Atkinson M R, Dixon A E and Damaskinos S 1992 Surface-profile reconstruction using reflection differential phase-contrast microscopy *Appl. Opt.* **31** 6765–71
Atkinson M R and Dixon A E 1994 Single-pinhole confocal differential phase contrast microscopy *Appl. Opt.* **33** 641–53
[44] Corle T R and Kino G S 1994 Differential interference contrast imaging on a real time confocal scanning optical microscope *Appl. Opt.* **29** 3769–74
[45] Juskaitis R and Wilson T 1992 Differential CSM with a two-mode optical fibre *Appl. Opt.* **31** 898–902
[46] Kino G S and Chim S S C 1990 Mirau correlation microscope *Appl. Opt.* **29** 3775–83

[47] Kimura S and Wilson T 1991 Confocal scanning optical microscope using single-mode fibre for signal detection *Appl. Opt.* **30** 2143–50

Gan X, Gu M and Sheppard C J R 1992 Fluorescent image formation in the fibre-optical confocal scanning microscope *J. Mod. Opt.* **39** 825–34